

COMPUTATIONAL HOMOGENISATION AND FAILURE MODELLING OF PERIODIC COMPOSITES

L.HARISH

**A Dissertation Submitted to
Indian Institute of Technology Hyderabad
In Partial Fulfilment of the Requirements for
The Degree of Master of Technology**



भारतीय प्रौद्योगिकी संस्थान हैदराबाद
Indian Institute of Technology Hyderabad

**Department of Civil Engineering
Indian Institute of Technology Hyderabad**

June, 2012

Declaration

I declare that this written submission represents my ideas in my own words, and where others' ideas or words have been included, I have adequately cited and referenced the original sources. I also declare that I have adhered to all principles of academic honesty and integrity and have not misrepresented or fabricated or falsified any idea/data/fact/source in my submission. I understand that any violation of the above will be a cause for disciplinary action by the Institute and can also evoke penal action from the sources that have thus not been properly cited, or from whom proper permission has not been taken when needed.



(Signature)

HARISH L

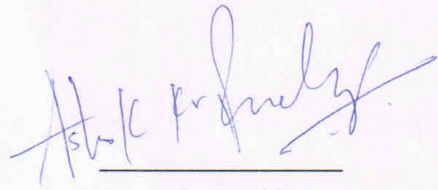
(- Student Name -)

CE10M03

(Roll No)

Approval Sheet

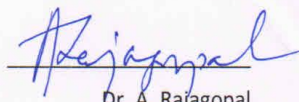
This thesis entitled "Computational homogenization and failure modelling of periodic composite"
by Harish.L is approved for the degree of Master of Technology from IIT Hyderabad



Dr. Ashok Pandey
Examiner



Prof. KVL Subramaniam
Examiner



Dr. A. Rajagopal
Adviser & Chairman

Acknowledgement

I would like to express my sincere gratitude to my thesis advisor Dr. A.Rajagopal without his support this work would have not been possible. It has been a wonderful experience working with him. All the learnings from this association will be of great help to me in my future endeavours.

I am extremely thankful to the Prof K.V.L Subramaniam, Dr.B.Umashankar, Dr.S.Sireesh of the Indian Institute of Technology Hyderabad, who have taught me and made my journey from a student to an engineer a memorable one. It was a pleasure to be associated with the civil cae lab of the Civil Department.

I would like to thank all my friends: Mahender kumar, Nitin chauhan, Sahith Gali, Umesh.B for their kind support.

Dedicated to
My parents, friends and professors

Abstract

Masonry and composite laminates are periodic in nature in their own plane. Masonry is a composite material made of units and mortar, normally arranged periodically. The combined action of brick and mortar will exhibit different directional properties. Finding the orthotropic properties or effective material properties from the individual material constituents is called the homogenisation. Less computational cost, user friendly mesh, and flexible to apply for large structures are advantages while using the homogenised properties. In this study we find the homogenised properties for unstrengthen masonry and also strengthened masonry using CFRP (inserted in bed joints). For composite laminates, homogenised properties can be found from modified rule of mixture.

The behaviour of a composite material under external loads is often quite different from that of an isotropic material. Modelling of damage in such materials is a complex problem because of the existence of several failure mechanisms at various length scales, e.g., fibre breakage, fibre-matrix debond, matrix cracks and delamination. This poses a need for understanding the damage mechanics thoroughly at various length scales. Hence, it is impossible to create a generalized damage model by simply observing the macro-level behaviour of the composite laminate. So, the analysis of composites needs to be a multi-scale one, where, the effective field variables at each scale are obtained from the homogenization of the field variables defined at a lower scale. Here Multi continuum theory and phase degradation approach was proposed to found the failure or damage of composite laminate at micro level when the loads are applied at the macro level. And also damage of the discrete masonry wall was predicted using the concrete damage plasticity material model in Abaqus 6.9 version.

List of Symbols

Σ	Macro average stress
Ω	Portion of masonry
S	Domain(cell)
σ	Stress field
δS	Boundary of basic cell
$\varepsilon(\mathbf{u})$	Strain field
\mathbf{u}^p	Periodic displacement field
\mathbf{u}	Strain periodic
E	Mean strain tensor of the cell
\mathbf{n}	Normal vector
\mathbf{c}	Fourth order tensor
V	Volume of the basic cell
A^r	Area of generic element
m	Number of elements
F_j	Resulting force
$\bar{\sigma}_j^r$	Average stress value for generic element
$\bar{\varepsilon}_j^r$	Average strain value for generic element
\bar{S}_{ij}	Compliance coefficients
\bar{C}_{ij}	Stiffness coefficients
G_f	Fracture energy
G_c	Compressive fracture energy
G_f^I	Mode I fracture energy
G_f^{II}	Mode II fracture energy

f_{mo}	Mortar compressive strength
$\tilde{\varepsilon}_t^{pl}$ and $\tilde{\varepsilon}_c^{pl}$	Equivalent plastic strains
d_t and d_c	Damage variable
E_0	Initial elastic stiffness
$\tilde{\varepsilon}_t^{ck}$	Tensile cracking strain
$\tilde{\varepsilon}_c^{in}$	Compressive inelastic strain
I_1, I_2, I_3, I_4, I_5	Invariants
A_{if} and A_{jm}	Coefficients and functions of strength parameters
σ_{vmc}^m	Critical von Mises stresses for matrix
μ	Pressure sensitivity of the matrix
T	Transformation matrix
$[A_m]$ and $[A_f]$	Amplification factors for matrix and fibre respectively
V_f	Fibre volume fraction

List of figures

- Figure 1.1** (a) Periodic composite of masonry (b) Periodic composite of unidirectional composite
- Figure 1.2** failures of the masonry walls due to earthquake
- Figure 1.3** Basic cell for masonry and objectives of homogenisation
- Figure 2.1** Different kinds of stone masonry: (a) rubble masonry; (b) ashlar masonry;(c) coursed ashlar masonry
- Figure 2.2** Different arrangements for brick masonry: (a) stack bond; (b) stretcher bond
- Figure 2.3** Modelling of masonry structures (a) masonry sample; (b) detailed micro modelling; (c) simplified micro-modelling; (d) macro modelling.
- Figure 2.4** Basic cell for masonry and objectives of homogenisation
- Figure 2.5** Macroscopically homogeneous stress state test [testing set-up from Dhanasekar et al. (1982)].
- Figure 2.6** Escher-like picture illustrating the concept of macroscopic homogeneity.
- Figure 3.1** Definition of masonry axes and of chosen micro mechanical model
- Figure 3.2** Modal dimensions of RVE's
- Figure 3.3** Finite element model-mesh
- Figure 3.4** FEA results for different stiffness ratios for RVE1: (a) Young's moduli (b) Poisson's ratio and (c) shear moduli.
- Figure 3.5** FEA results for different stiffness ratios for RVE2: (a) Young's moduli (b) Poisson's ratio and (c) shear moduli.
- Figure 3.6** FEA results for different stiffness ratios for RVE1: (a) Young's moduli and (b) shear moduli.
- Figure 3.7** FEA results for different stiffness ratios for RVE2: (a) Young's moduli and (b) shear moduli.

- Figure 3.8** (a) FE model of RVE with CFRP (b)FE discretization
- Figure 3.9** FEA results for different stiffness ratios of (a) young's modulus in x direction(b) young's modulus in Y direction (c) young's modulus in Z direction
- Figure 3.10** FEA results for different stiffness ratios of (a) shear modulus in XY(b) shear modulus in YZ (c) shear modulus in ZX
- Figure 4.1** Modelling of masonry structures (a) masonry sample; (b) detailed micro modelling; (c) simplified micro-modelling; (d) macro modelling
- Figure 4.2** Typical behaviour of quasi-brittle materials under uniaxial loading (a) tensile loading); (b) compressive loading
- Figure 4.3** Behaviour of masonry under shear (c denotes the cohesion). [Lourenco 2006]
- Figure 4.4** Typical experimental stress-displacement diagrams for $500 \times 250 \times 600$ [mm^3] prisms of solid soft mud brick
- Figure 4.5** Typical experimental stress-displacement diagrams (a) failure occurs with a stepped crack through head and bed joints; (b) failure occurs vertically through head joints and units.
- Figure4.6** Response of concrete to uniaxial loading in compression
- Figure 4.7** Response of concrete to uniaxial loading in (a) tension and (b) compression
- Figure 4.8** masonry wall model (b) FE discretization of masonry
- Figure 4.9** (a) stress-displacement curve for masonry under tensile loads (b) stress-strain curve for masonry in compressive loads
- Figure 4.10** (a) damage distribution of masonry wall (b) load vs. displacement graph for masonry
- Figure 4.11** Three-dimensional unit cell for reinforced composite

- Figure 4.12** Matrix failure criterion
- Figure 4.13** stress distribution in a carbon/epoxy lamina subjected to a unit applied stresses: (a)xx-stress and (b) yy-stress
- Figure 4.14** (a) open hole tension specimen (b) FE discretization of the quarter part of OHT specimen
- Figure 4.15** Damage progression for ply-1 and ply-2 of laminated composite (-30/30/-30/30) (a) 1st ply (30 deg) (b) 2nd ply (-30 deg)

List of the tables

- Table 4.1** Matrix properties (3501-6)
- Table 4.2** Fibres properties (3501-6)

Contents

Declaration.....	ii
Approval sheet	iii
Acknowledgements.....	iv
Abstract.....	vi
List of symbols.....	vii
List of figures.....	ix
List of tables.....	xi
Chapter 1: Introduction.....	1
1.1 Homogenisation and Failure modelling of periodic composite.....	1
1.2 Laminated composite modelling as a periodic composite.....	5
1.3 Objective of the study.....	7
1.4 Outline of the thesis.....	7
Chapter 2: Literature survey.....	9
2.1 Micromechanics of masonry.....	9
2.2 Homogenisation background.....	12
2.3 Homogenisation theory for periodic media.....	14
2.4 Micromechanics based failure theory for composite laminates.....	17
Chapter 3: Computational homogenisation.....	19
3.1 Introduction.....	19
3.2 Micro-mechanical model.....	19
3.3 Stress-prescribed analysis.....	22
3.3.1 Homogenised elastic compliances.....	22
3.3.2 Homogenised properties results from RVE's.....	24
3.3.3 Effect of mortar modulus.....	26
3.4 Strain prescribed analysis.....	27
3.4.1 Homogenised elastic stiffness.....	27

3.4.2 Homogenised properties results from RVE's.....	28
3.5 Homogenisation of masonry strengthening by CFRP.....	29
3.6 Conclusion.....	33
Chapter 4: Failure modelling of periodic composites.....	34
4.1 Introduction.....	34
4.2 Behaviour of masonry in different aspects.....	36
4.2.1 Softening Behaviour.....	36
4.2.2 Uniaxial compressive behaviour.....	38
4.2.3 Uniaxial tensile Behaviour.....	38
4.3 Damage modelling of masonry	40
4.3.1 Constitutive model.....	40
4.4 Failure modelling of masonry under lateral displacements.....	44
4.5 Multi scale failure theory for composite laminate.....	47
4.6 Multi-continuum failure criteria.....	47
4.6.1 Fibre failure.....	48
4.6.2 Matrix failure.....	49
4.7 Laminate analysis.....	51
4.8 Micromechanics solutions.....	51
4.9 Phase degradation approach.....	52
4.10 Open-hole Tension (OHT) specimen.....	54
4.10.1 Damage progression in open hole tension specimen.....	55
4.11 Conclusion.....	56
Chapter 5: Conclusions.....	57
5.1 Conclusion and summary.....	57
References.....	59

Chapter 1

Introduction

1.1 Homogenisation and failure modelling of periodic composite

Masonry has been largely utilized in the history of architecture, in the past. Despite their present uncommon use in new buildings, they still represent an important research topic due to several applications in the framework of structural engineering, with particular reference to maintaining and restoring historical and monumental buildings.

Hence, even if new materials (for example the reinforced concrete) are wider spread than masonry ones, the unquestionable importance of a lot of real masonry estate require researcher's particular attention for this kind of structures. Therefore, in order to design an efficient response for repairing existing masonry structures, a large number of theoretical studies, experimental laboratory activities and computational procedures have been proposed in scientific literature.

Masonry is a heterogeneous medium which shows an anisotropic and inhomogeneous behaviour in nature. In particular, the inhomogeneity is due to its biphasic composition and, consequently, to the different mechanical properties of its constituents such as mortar and natural or artificial blocks. The anisotropy is, instead, due to the different masonry patterns since the mechanical response is affected by the geometrical arrangement of the constituents. Basically, in literature, two approaches are usually taken into account for materials which have a heterogeneous micro-structure: the heuristic approach and the thermodynamical approach. In the former, a aprioristic hypotheses on the dependence of the constitutive response on a certain number of parameters are considered and the material's mechanical behaviour is obtained by such hypotheses and by experimental tests. This approach is particularly used in non-linear field, where structural analyses are employed (Heyman, 1966). Our attention was focused on the latter approach. It extends the use of the homogeneous classical elasticity to heterogeneous materials by replacing the elastic constants of the classical homogeneous theory with the effective elastic ones, which average the actual inhomogeneous

properties of the medium. Hence, such approach yields the overall compliance tensor and the overall stiffness tensor in a mathematical framework by means of mathematical operations of volume averaging and thermo dynamical consistency. In this way, starting from the concepts of the average strain for prescribed macro stress and of the average stress for prescribed macro strain, the global behaviour is provided from the masonry micro-structure geometry and from the known properties of the individual constituents. So in masonry the effective properties or homogenised properties are found from the micromechanics of RVE's (Representative Volume Element) using the average theorems. In the unidirectional composite or composite laminate, the effective properties or homogenised properties are found from the micromechanics of masonry using the rule of mixture or modified rule of mixture.

Figure 1.1 shows the Masonry and composite laminates are three dimensional composite medium admitting only two directions of periodicity in its own plane.

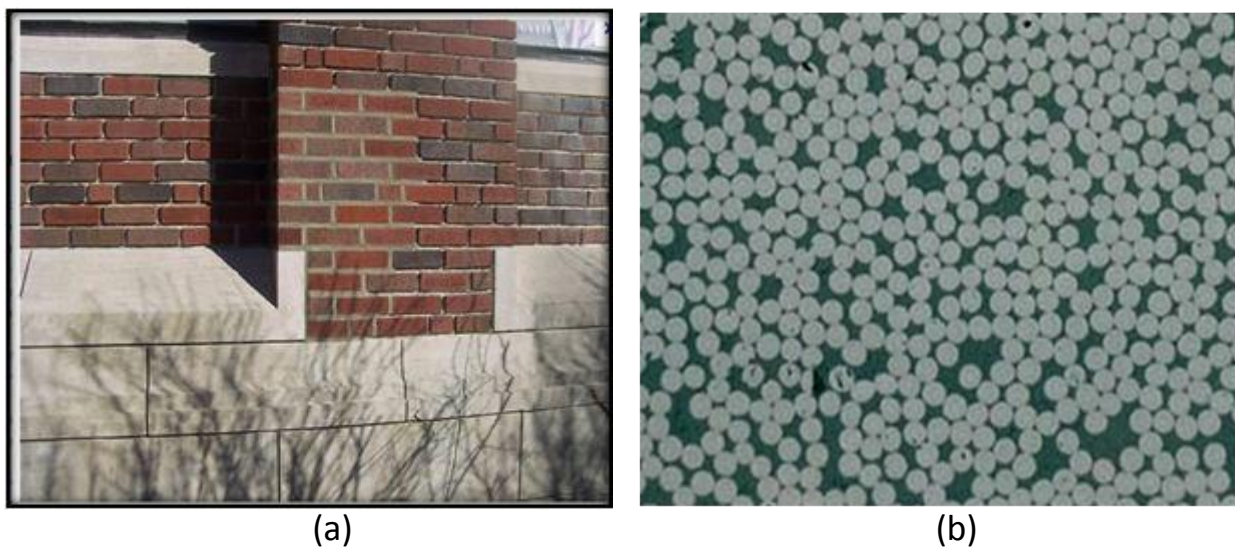


Figure 1.1 (a) Periodic composite of masonry (b) Periodic composite of unidirectional composite[19]

In this framework, advanced numerical strategies based on the finite element method have been developed.

As one of the oldest building materials, masonry was not only used in many magnificent historical structures all over the world but is still used in various new constructions. The need of structural

rehabilitation and strengthening of ancient masonry structures motivated studies to better understand the deformation and failure mechanism of masonry structures. Unreinforced masonry structures are particularly vulnerable to earthquake excitations due to the fact that the integrity of these structures relies mainly on the joining material between masonry blocks which is apt to crack when subjected to tension caused by earthquake lateral forces. The recent earthquakes in various countries have caused great damage and destruction to masonry bridges, religious temples, and other monumental buildings.

Some example of the collapse of masonry building of shear walls after an earthquake are shown in Figure 1.2 Earthquake Damage, Northern Iran, June 21, 1990 has revealed that the masonry structures experienced the worst damage during the earthquake. These incidents further enlightened the need to have a better understanding of the behaviour of masonry structure through experimental and numerical studies. The practical need is motivated to research on modelling masonries subjected to lateral loads.



Figure 1.2 failures of the masonry walls due to earthquake [Geo hazard index html]

In spite of the simplicity associated with building in masonry, the analysis of the mechanical behaviour of masonry constructions remains a true challenge.

Basically, two different approaches have been used to model the masonry behaviour: the “micro-modelling” and the “macro-modelling” or ‘equivalent-material approach’. Selection of the approach depends upon the level of accuracy and the objective sought. The former approach models the actual geometry of both the blocks and mortar joints, adopting different constitutive models for the two components. Although this approach may appear very straightforward, its major disadvantage comes from the extremely large number of elements are required and the requirement of knowing the precise layout of each brick. A three-dimensional micro-modelling analysis of a masonry panel with only a very simple geometry would require a large number of elements in order to enable accurate modelling of each joint and block unit. Hence, the use of micro-models is impossible / impractical for the global analysis of entire buildings or bridges. In addition, the actual distribution of blocks and joints might be impossible to detect unless many investigations are performed.

To overcome this computational difficulty, the macro-modelling approach, in which masonry is modelled by an equivalent continuous material, is used for structural analysis. The macro-models do not make a distinction between individual blocks and mortar joints, smearing the effect of joint presence through the formulation of the constitutive relations of an equivalent material. Such a constitutive model has to reproduce an average mechanical behaviour of small masonry panel. The main advantages of the macro approach are the enormous reduction of the computational cost, which makes possible the numerical analyses of complex structures such as bridges and buildings. The macro approach makes it feasible to analyse any masonry structure without detailed knowledge of the layout of individual bricks.

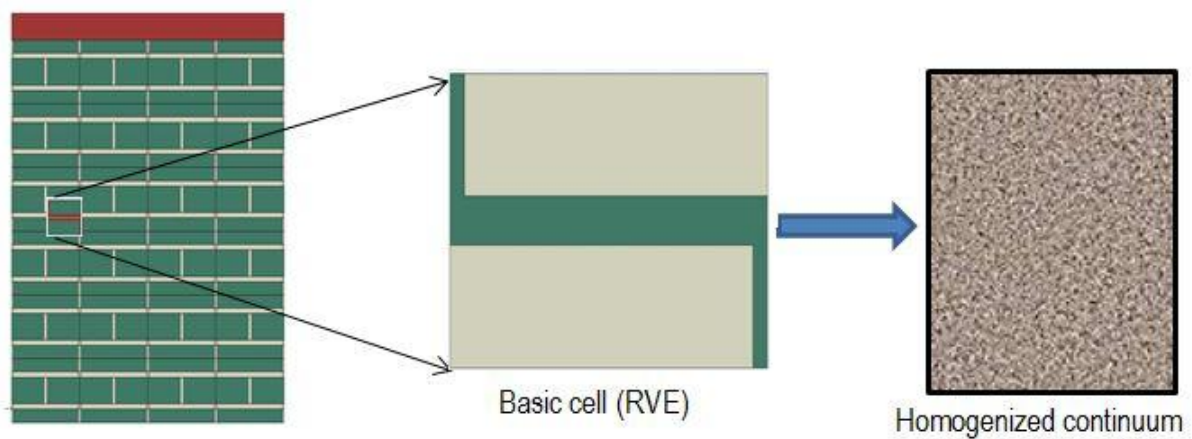


Figure 1.3 Basic cell for masonry and objectives of homogenisation

Based on the above comparison discrete masonry wall is created based on individual constituent properties of brick and mortar, and predicted damage of wall under lateral loads or displacements. Based on the above comparison for the both micro-modelling and macro-modelling approaches, a two stage modelling strategy is suitable. First, homogeneous equivalent material properties are obtained by using micro-modelling approaches. Specifically, the micromechanics model called Finite element analysis will be used to achieve the equivalent continuous material for small masonry panel. Figure 2.3 shows the part of the masonry wall taken as RVE to get homogenised properties or equivalent properties using the microanalysis of average theorem. Then, the second one discrete wall is modelled using constituent properties of brick and mortar to predict the damage of wall under lateral loads and lateral displacements.

1.2 Laminated composite modelling as a periodic composite

Because of composite structures offer a number of advantages over conventional metallic materials, including lightweight and better corrosion resistance, there is an increasing tendency in the development of new aircraft towards an even more widespread use of composites. For instance, Boeing's 7E7 aircraft will contain 50% by weight of carbon fibre reinforced composites. Given the fact that there are numerous examples where composite materials are being successfully used in primary load-bearing structures, one might logically conclude that design procedures (including strength prediction) for fibre reinforced composites are fully mature. To the contrary, even at the lamina or laminate level, there is a lack of evidence to show that any of the failure criteria developed so far could provide accurate and meaningful predictions of failure beyond a very limited range of circumstances. Therefore it remains persistent difficulty to accurately predict laminate failure under combined loading by using either unidirectional composite (ply) data or with basic constituent material properties. This has been the main motivation for major worldwide failure exercise over the past decade.

To accelerate the insertion of composite materials/structures into application and to reduce the associated certification cost, aircraft structures are moving towards certification by analysis

supported by test and demonstration. To this end an advanced predictive capability is required that is able to accurately assess the damage tolerance and durability of fibre-reinforced composites. In the context of through-life support and management of composite structures, a predictive capability would also improve the design and qualification of repairs. Because the failure process of composite structures involves failures at multiple length scales, including the microscopic scale (fibre, matrix and fibre/matrix interface), the macroscopic scale (structure), a predictive capability would need to deal with the onset of microscopic failures, their progression to the mesoscopic scale, and the ultimate coalescence into macroscopic damage causing structural failure.

Recently the strain invariant failure theory (SIFT) has emerged as a promising predictive method for composite laminates. Compared to the traditional composite failure theories, including the Tsai-Wu interactive failure theories, and the physically based failure criteria by Hashin and Rotem, the SIFT method represents a first step towards multi-scale modelling that attempts to link structural failure to events at the fibre-resin level. In this context, SIFT is similar to the multi-continuum theory, although SIFT does appear to have the advantage that the critical strain invariants determined from lamina data were reported to correlate well with net resin properties. The important feature of the SIFT provides a basis for an accelerated durability assessment methodology.

In the strain-invariant failure theory, the matrix and fibre phases are characterised by separate failure criteria. Matrix is considered to fail either under dilation mode or shear mode, while fibre is assumed to fail by shear distortion. Consequently, composite failure is completely characterised by three critical invariants. However, such an approach does not capture the micro-buckling failure mode under compression and therefore would over-predict the strength of compression failure which is often dominated by micro-buckling. Furthermore, SIFT was essentially developed to determine the onset of failures in composites, rather than the ultimate load carrying capacity. Nevertheless, attempts have been made to extend SIFT to predict the maximum load-carrying capacity by using a maximum energy retention method.

The purpose of study is to present a multi-scale failure theory that accounts for the pressure-sensitivity of polymer matrix, fibre fracture under tension, and fibre micro buckling under compression. Similar to the SIFT, the present approach treats a laminate as a stack of transversely isotropic plies. At the ply level, matrix failure is due to the combination of dilation and distortion, while the fibres can fail either by micro-buckling or by distortion. Damage progression through plies is simulated by judiciously degrading the constituent stiffness, hence the ply stiffness.

1.3 Objectives of the study

- ❑ To formulate and implement a computational homogenization scheme for periodic composites.
 - ❖ To implement the above procedure for
 - a) Unreinforced masonry
 - b) Masonry strengthened with CFRP
 - c) Laminated composites.
- ❑ To formulate and implement a failure model for periodic composites.
 - ❖ To implement a plasticity based damage model for masonry failure
 - ❖ To implement a phase degradation approach for modeling failure in laminated composite.

1.4 Outline of the thesis

The present work is outlined as follows:

1. The first chapter introduces the Homogenisation of the periodic composite from the micromechanical analysis and the briefly gives an idea of failure modelling of periodic composite.
2. In the next chapter deals the homogenisation theory from the literature survey is presented and brief literature survey on failure modelling of periodic composite.

3. The third chapter deals results from homogenisation of masonry based on stress prescribed and strain prescribed analysis of volume averaging theorem, and results based on homogenisation of masonry with CFRP based on stress prescribed and strain prescribed analysis of volume averaging theorem.
4. In the final chapter, plasticity damage model for masonry failure is presented and phase degradation approach for modelling failure in laminated composites is presented.

Chapter 2

Literature survey

2.1 Micromechanics of masonry

Masonry is the oldest building material that is still currently used in the building industry. Masonry is a heterogeneous material composed of units and mortar joints. Irregular stones, ashlar, adobes, bricks and blocks have been used as units. The units can be joined together using mortar (commonly clay, lime or cement based mortar) or just by simple superposition. With these two components, a large number of arrangements can be accomplished, generated from the different combinations of units and joints. A possible classification of stone masonry is shown in Figure 2.1 and the most used combinations are illustrated in Figure 2.2

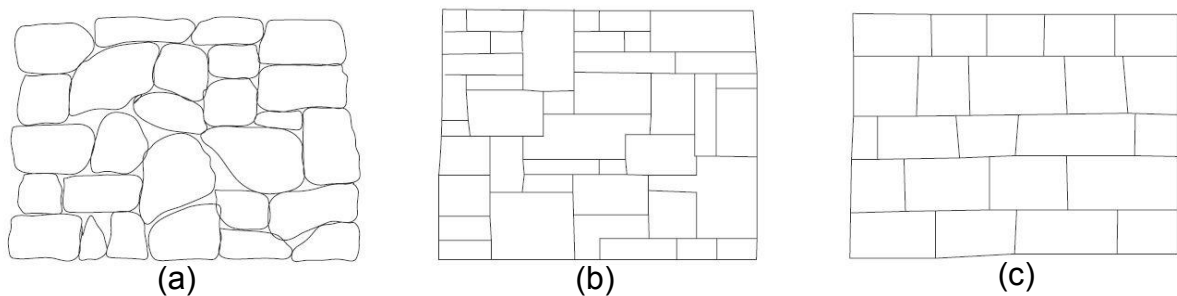


Figure 2.1 Different kinds of stone masonry: (a) rubble masonry; (b) ashlar masonry; (c) coursed ashlar masonry (Lourenço, 1998).

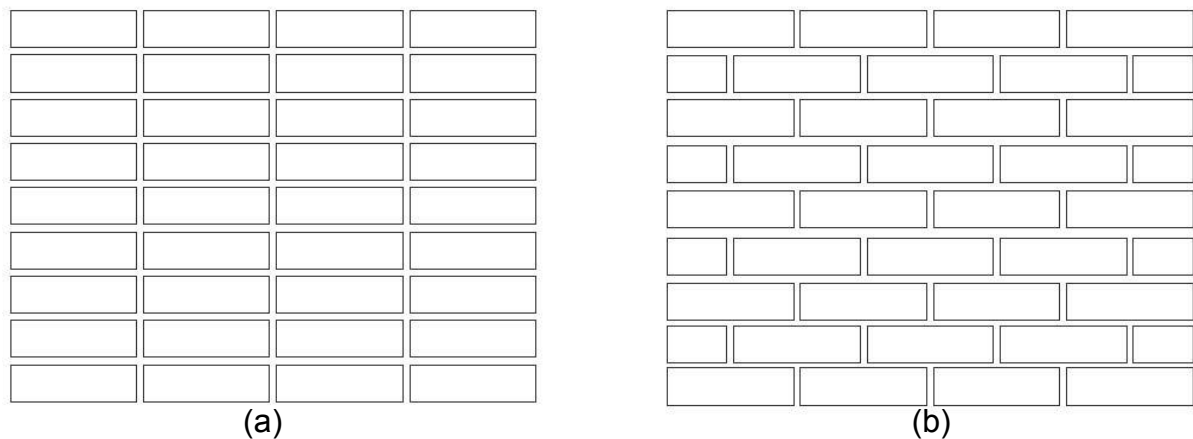


Figure 2.2 Different arrangements for brick masonry: (a) stack bond; (b) stretcher bond

In spite of the simplicity associated with building in masonry, the analysis of the mechanical behaviour of masonry constructions remains a true challenge. Masonry is a material that exhibits distinct directional properties due to the mortar joints, which act as planes of weakness. Consequently, masonry structures display shows an anisotropic and inhomogeneous nature. In particular, the inhomogeneity is due to the different mechanical properties of its constituents, mortar and unit. The anisotropy is due to the different masonry patterns since the mechanical response is affected by the geometrical arrangement of the constituents. In general, the approach towards its numerical representation can focus on the micro-modelling of the individual components, i.e., unit (brick, block, etc.) and mortar, or the macro-modelling of masonry as a composite (Rots 1991).

Depending on the level of accuracy and simplicity desired, it is possible to use following modelling strategies as described in Figure 2.3

- Detailed micro modelling- units and mortar joints are represented by continuum elements whereas the unit mortar interface represented by discontinuous elements;
- Simplified micro modelling- expanded units are represented by continuum elements whereas the behaviour of the mortar joints and unit mortar interface is lumped in discontinuous elements;
- Macro modelling- units, mortar and unit-mortar interface are smeared out in the continuum.

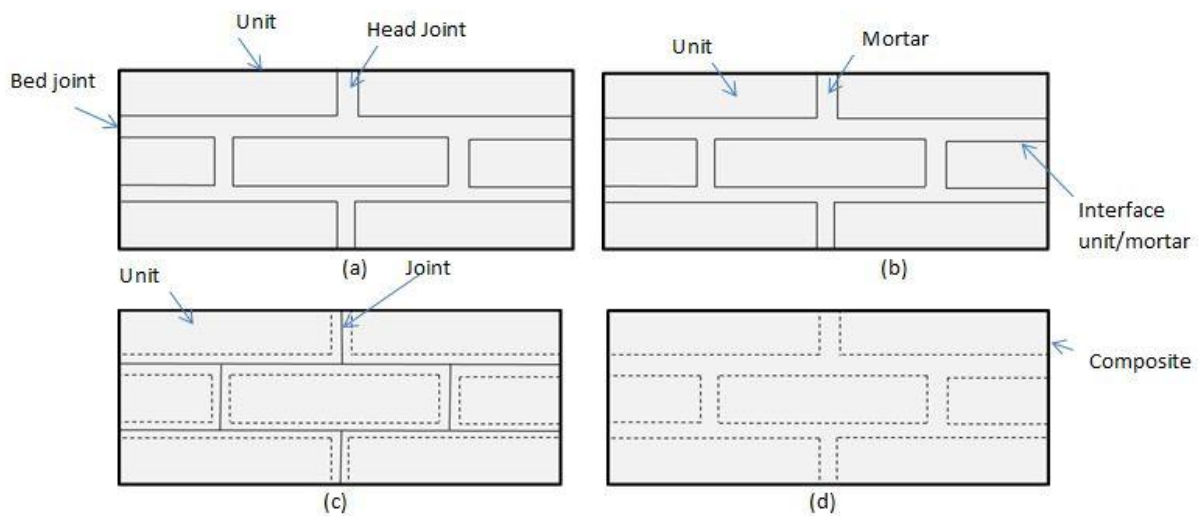


Figure 2.3 Modelling of masonry structures (a) masonry sample; (b) detailed micro modelling; (c) simplified micro-modelling; (d) macro modelling.

In the first modelling, Young's modulus, Poisson's ratio and, optionally, inelastic properties of both unit and mortar are taken into account. The interface represents a potential crack/slip plane with initial dummy stiffness to avoid interpenetration of the continuum. This enables the combined action of unit, mortar and interface to be studied. In the second modelling, each joint, consisting of mortar and the two unit-mortar interfaces, is lumped into an "average" interface while the units are expanded in order to keep the geometry unchanged. Masonry is thus considered as a set of elastic blocks bonded by potential fracture/slip lines at the joints. Accuracy is lost since Poisson's effect of the mortar is not included. The third approach does not make a distinction between individual units and joints but treats masonry as a homogeneous anisotropic continuum [2]. One modelling strategy cannot be preferred over the other because different application fields exist for micro- and macro-models. Micro-modelling studies are necessary to give a better understanding about the local behaviour of masonry structures. This type of modelling applies notably to structural details, but also to modern building systems like those of concrete or calcium-silicate blocks, where window and door openings. Macro-models are applicable when the structure is composed of solid walls with sufficiently large dimensions so that the stresses across or along a macro-length will be essentially uniform. Clearly, macromodeling is more practice oriented due to the reduced time and memory

requirements as well as a user-friendly mesh generation. This type of modelling is most valuable when a compromise between accuracy and efficiency is needed.

Accurate micro- or macro-modelling of masonry structures requires a thorough experimental description of the material. However, the properties of masonry are influenced by a large number of factors, such as material properties of the units and mortar, arrangement of bed and head joints, anisotropy of units, dimension of units, joint width, quality of workmanship, and degree of curing, environment and age.

2.2 Homogenisation background

Masonry is a composite material made of units and mortar, normally arranged periodically. Utilising the material parameters obtained from experiments and the actual geometry of both components, viz. units (e.g. bricks, blocks or stones) and joints, it is possible to numerically reproduce the behaviour of masonry structures, see e.g. Lourenco and Rots (1997). Nevertheless, the representation of each unit and each joint becomes impractical in case of real masonry structures comprising a large number of units.

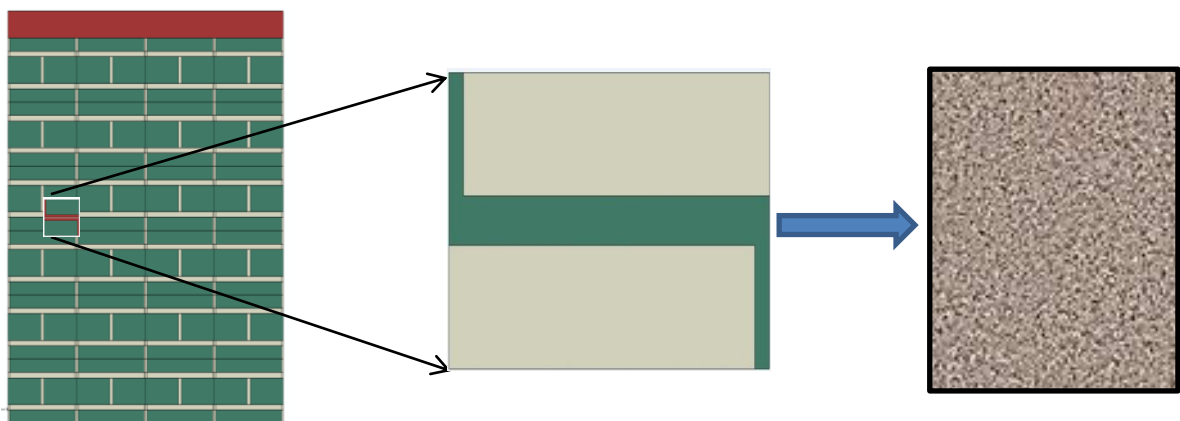


Figure 2.4 Basic cell for masonry and objectives of homogenisation

The alternative is to describe the composite behaviour of masonry in terms of macro or average stresses and strains so that the material can be assumed homogeneous. This problem can be approached, basically, from two directions. A possible direction is to gather extensive

experimental data that can be used confidently in the analyses. It is stressed that the results are limited to the conditions under which the data are obtained. This approach, which aims at describing the behaviour of the composite from the geometry and behaviour of the representative volume element (or basic cell, see Figure 2.4), grants us a predictive capability.

The techniques of homogenisation (Bakhvalov and Panasenko, 1989) are currently becoming increasingly popular among the masonry community. A method that would permit to establish constitutive relations in terms of averaged stresses and strains from the geometry and constitutive relations of the individual components would represent a major step forward in masonry modelling. Given the difficult geometry of the masonry basic cell, a close-form solution of the homogenisation problem seems to be impossible, which leads, basically, to three different lines of action.

The first, very powerful approach is to handle the brickwork structure of masonry by considering the salient features of the discontinuum within the framework of a generalised/Cosserat continuum theory. This elegant and efficient solution (Besdo, 1985; Muhlhaus, 1993) possesses some inherent mathematical complexity and has not been adopted by many researchers, even though being capable of handling the unit–mortar interface and true discontinuum behaviour. The step towards the practical application of such an approach is still to be done.

A second approach (Anthoine, 1995, 1997; Urbanski et al., 1995) is to apply rigorously the homogenisation theory for periodic media to the basic cell, i.e. to carry out a single step homogenisation, with adequate boundary conditions and exact geometry. It is stressed that the unit–mortar interface has not yet been accounted for by researchers. The complexity of the masonry basic cell implies a numerical solution of the problem, which has been obtained using the finite element method. The theory was thus used by the cited authors to determine macro-parameters of masonry and not, actually, to carry out analysis at the structural level. In fact, the rigorous application of the homogenisation theory for the non-linear behaviour of the complex masonry basic cell implies solving the problem for all possible macroscopic loading histories, since the

superposition principle does not apply anymore. Thus, the complete determination of the homogenised constitutive law would require an infinite number of computations.

The third approach can be considered as an “engineering approach”, aiming at substituting the complex geometry of the basic cell by a simplified geometry so that a close-form solution of the homogenisation problem is possible. Keeping in mind the objective of performing analysis at the structural level, Pande et al. (1989), Maier et al. (1991) and Pietruszczak and Niu (1992) introduced homogenisation techniques in an approximate manner. The homogenisation has generally been performed in two steps, head (or vertical) and bed (or horizontal) joints being introduced successively. In this case masonry can be assumed to be a layered material, which simplifies the problem significantly. Lourenco (1996) further developed the procedure, presenting a novel matrix formulation that allows a much clearer implementation of linear elastic homogenisation algorithms and also a relatively simple extension to non-linear behaviour.

The present study a new micro-mechanical model, for masonry in stretcher bond, to overcome the limitations of the standard two-step homogenisation by a more detailed simulation of the interactions between the different internal components of the basic cell. The model can still be considered as an engineering approach, in which an ingenious observation of the behaviour of masonry leads to the simulation of additional internal deformation mechanisms of the joints that become more and more important for increasing unit/mortar stiffness ratios. At this stage, the unit–mortar interface is not considered in the model.

2.3 Homogenization theory for periodic media

Suppose now that a portion Ω of masonry is subjected to a globally homogeneous stress state. A stress state is said to be globally or macroscopically homogeneous over a domain Ω if all cells within Ω undergo the same loading conditions. This can be approximately achieved with an experimental set-up designed to apply any biaxial principal stress state to a panel (Dhanasekar *et al.*, 1982). The shear stress component is then obtained by selecting the proper lay-up angle of the

specimen (Fig. 5). The approximation is due to perturbations near the boundary; a cell lying near the boundary $\delta\Omega$ of the specimen is not subjected to the same loading as one lying in the centre. However, on account of the Saint- Venant principle, cells lying far enough from the boundary are subjected to the same loading conditions and therefore deform in the same way. In particular, two joined cells must still fit together in their common deformed state, just like in a picture of Escher (Fig. 6). In mechanical terms, this means that, when passing from a cell to the next one, (i) the stress vector $\boldsymbol{\sigma} \cdot \mathbf{n}$ is continuous; (ii) strains are compatible, i.e. neither separation nor overlapping occurs. Since passing from a cell to the next one which is identical, also means passing from a side to the opposite one in the same cell S , condition (i) becomes

Stress vectors $\boldsymbol{\sigma} \cdot \mathbf{n}$ are opposite on opposite sides of δS

because external normal \mathbf{n} are also opposite. Such a stress field $\boldsymbol{\sigma}$ is said to be periodic on δS , whereas the external normal \mathbf{n} and the stress vector $\boldsymbol{\sigma} \cdot \mathbf{n}$ are said to be anti-periodic on δS .

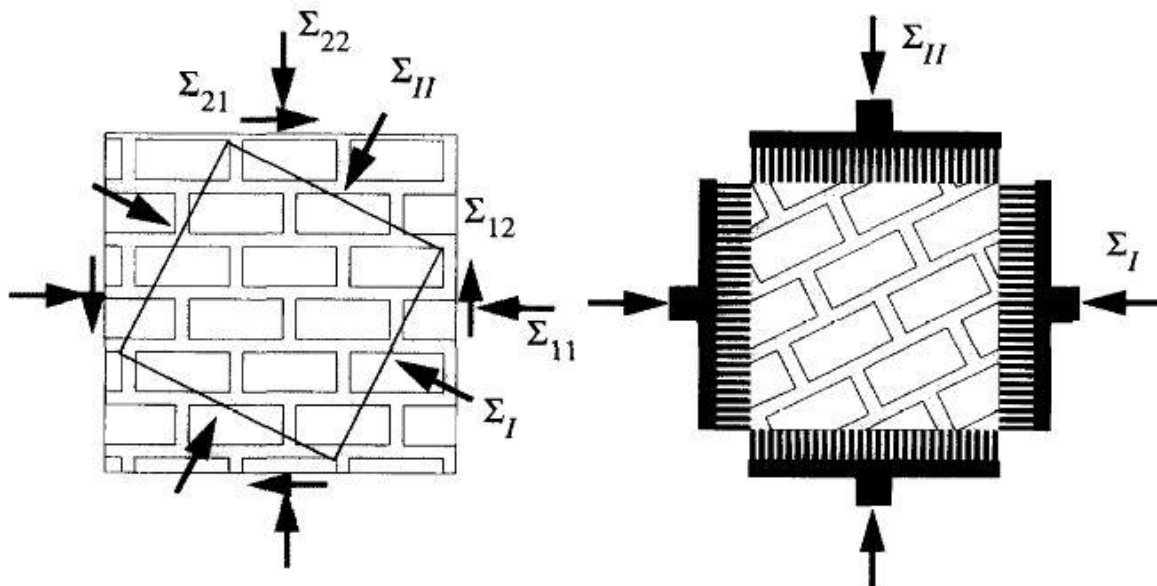


Figure 2.5 Macroscopically homogeneous stress state test [testing set-up from Dhanasekar et al. (1982)].

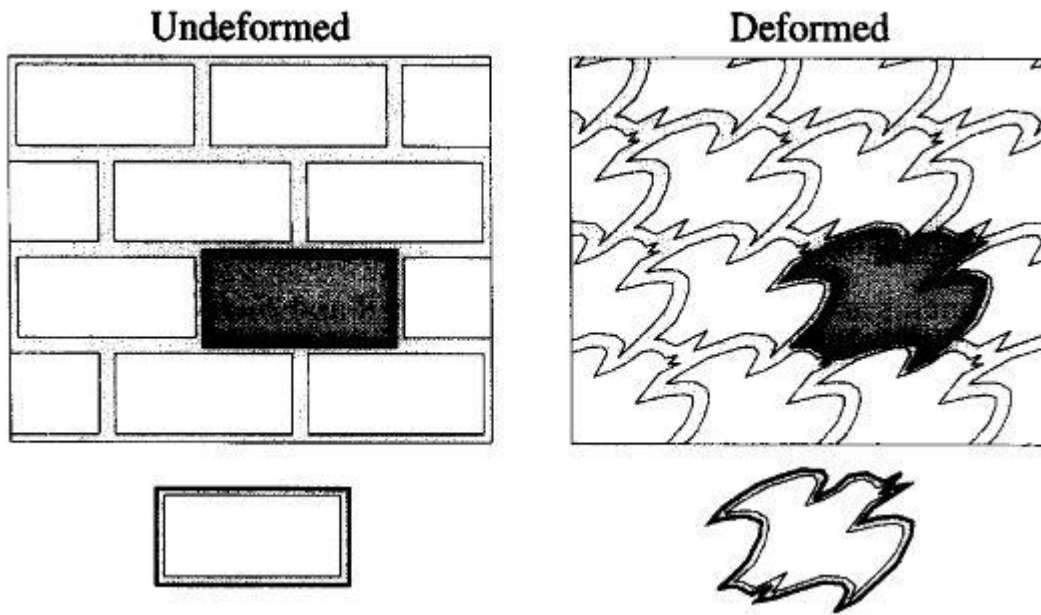


Figure 2.6 Escher-like picture illustrating the concept of macroscopic homogeneity.[1]

Let us consider the problem of a masonry specimen subjected to a macroscopically homogeneous stress state Σ . The previous discussion was devoted to the special conditions holding on the boundary δS of any cell S ; σ is periodic and u is strain-periodic. Those conditions make it possible to study the problem within a single cell rather than on the whole specimen. In order to find σ and u everywhere in a cell, equilibrium conditions and constitutive relationships must be added so that the problem to solve is

$$\text{div } \sigma = 0 \text{ on } S \text{ (No body forces)}$$

$$\sigma = f(\varepsilon(u)) \text{ (Constitutive law under plane stresses)}$$

$$\sigma \text{ periodic on } \delta S \text{ (} \sigma \cdot n \text{ anti-periodic on } \delta S)$$

$$u - \langle \varepsilon(u) \rangle \cdot x \text{ (periodic on } \delta S)$$

$$\langle \sigma \rangle = \Sigma, \Sigma \text{ given stress controlled loading,} \quad (2.1)$$

Where the constitutive law f is a periodic function of the spatial variable x since it describes the behaviour of the different materials in the composite cell. A problem similar to (2.1) is obtained when replacing the stress controlled loading by a strain controlled one

$$\langle \varepsilon(u) \rangle = E, E \text{ given.} \quad (2.1a)$$

In both cases, the resolution of (2.1) is sometimes termed “localization” because the local (microscopic) fields σ and $\varepsilon(u)$ determined from the global (macroscopic) quantity Σ or \mathbf{E} .

It is worth noting that, independently of the constitutive laws of the materials, the average procedure holds true in an energetic sense, i.e.

$$\langle \sigma : \varepsilon(u) \rangle = \langle \sigma \rangle : \langle \varepsilon(u) \rangle = \Sigma : E \quad (2.2)$$

Homogenization in linear elasticity:

Both constituents (brick and mortar) are now assumed linear elastic and perfectly bonded. Problem (1) with strain controlled loading reads

$$\text{div } \sigma = 0 \text{ on } S$$

$$\sigma = c : \varepsilon(u)$$

$$\sigma \cdot n \text{ anti-periodic on } \delta S$$

$$u - E \cdot x \text{ periodic on } \delta S, \quad (2.3)$$

Where \mathbf{E} is a given symmetric second-order tensor and c is the fourth-order tensor of elastic stiffnesses in plane stress. Writing (2.3) in terms of $u^p = u - E \cdot x$, and eliminating σ , the following system is obtained:

$$\text{div } (c : \varepsilon(u^p)) + \text{div } (c : E) = 0 \text{ on } S$$

$$c : (\varepsilon(u^p) + E) \cdot n \text{ anti periodic on } \delta S.$$

$$u^p \text{ periodic on } \delta S. \quad (2.4)$$

Note that the term $c : (\varepsilon(u^p) + E) \cdot n$ simply reduces to $c : \varepsilon(u^p) \cdot n$ if the material characteristics are continuous across the boundary δS . The solution of (2.4) is then the periodic displacement field inducing a periodic stress field and equilibrating the body forces \mathbf{f} induced by the uniform strain $(-E)$.

2.4 Micromechanics-Based Failure Theory for composite laminates

Huang [2001, 2004a, 2004b] developed a micromechanics-based failure theory so called “the bridging model”. The bridging model can predict the overall instantaneous compliance matrix of the lamina made from various constituent fibre and resin materials at each incremental load level and

give the internal stresses of the constituents upon the overall applied load. The lamina failure is assumed whenever one of the constituent materials attains its ultimate stress state. Using classical laminate theory (CLT), the overall instantaneous stiffness matrix of the laminate is obtained and the stress components applied to each lamina is determined. If any ply in the laminate fails, its contribution to the remaining instantaneous stiffness matrix of the laminate will no longer occur. In this way, the progressive failure process in the laminate can be identified and the laminate total strength is determined accordingly.

Multicontinuum theory (MCT) is numerical algorithm for extracting the stress and strain fields for a composites constituent during a routine finite element analysis [Mayes and Hansen, 2004a, 2004b]. The theory assumes: (1) linear elastic behaviour of the fibres and nonlinear elastic behaviour of the matrix, (2) perfect bonding between fibres and matrix, (3) stress concentrations at fibre boundaries are accounted for only as a contribution to the volume average stress, (4) the effect of fibre distribution on the composite stiffness and strength is accounted for in the finite element modelling of a representative volume of microstructure, and (5) ability to fail one constituent while leaving the other intact results in a piecewise continuous composite stress-strain curve. In MCT failure theory, failure criterion is separated between fibre and matrix failure and it is expressed in terms of stresses within composite constituent.

Gosse [Gosse and Christensen, 2001; Gosse, 1999] developed micromechanics failure theory which is based on the determination of fibre and matrix failure by using critical strain invariants. The theory is called strain invariant failure theory, abbreviated as SIFT. Failure of composite constituent is associated with one invariant of the fibre, and two invariants for the matrix. Failure is deemed to occur when one of those three invariants exceeds a critical value. For the past three years, SIFT has been tested to predict damage initiation in three-point bend specimen [Tay et al, 2005] and matrix dominated failure in I-beams, curved beams and T-cleats [Li et al, 2002; Li et al, 2003].

Chapter3

Computational homogenisation

3.1 Introduction

It has been seen that the FEM can be thought as a mathematical model able to include in it the continuum theories. Such method, in fact, overcomes the difficulties of the analysis of a continuum solid structural response by operating a discretization of the same continuum. This means, as already seen, that the solid is divided in to finite number of elements, whose structural behaviours are known. Such elements, when assembled with accurate relation laws among the nodes, are able to yield the global behaviour of the primitive solid, even if approximately. Obviously, the solution is as much close to the actual mechanical response as the mesh is refined. The goal of this chapter will be to show some computational analyses, carried out by means of the calculation code Abaqus 6.9 version.

This software offers a large number of appliances in a lot of engineering fields and it is just based on the mathematical F.E.M. model.

In the present study, the used micro-mechanical model and the effected analyses will be described. Since, in linear-elastic field, a numerical analysis can efficaciously replace an experimental test, such finite element analyses have been employed in order to compare the numerical results obtained by our proposed homogenization techniques with the literature data.

3.2 Micro-mechanical model

The micromechanics theory is to employ a representative volume element (RVE) to calculate the equivalent elastic constants and failure modes of masonry material with the help of finite element software Abaqus6.9. Both the units and mortar joints are idealized as isotropic material having their own properties such as modulus of elasticity and poissons ratio characteristics. Based on the numerical results, the equivalent material properties are used as the homogenized material properties in numerical simulation of a full masonry structure based on the continuum approach. It

is constituted by a periodic basic cell extracted from a single leaf masonry wall in stretcher bond, as shown in the figure 3.1 below

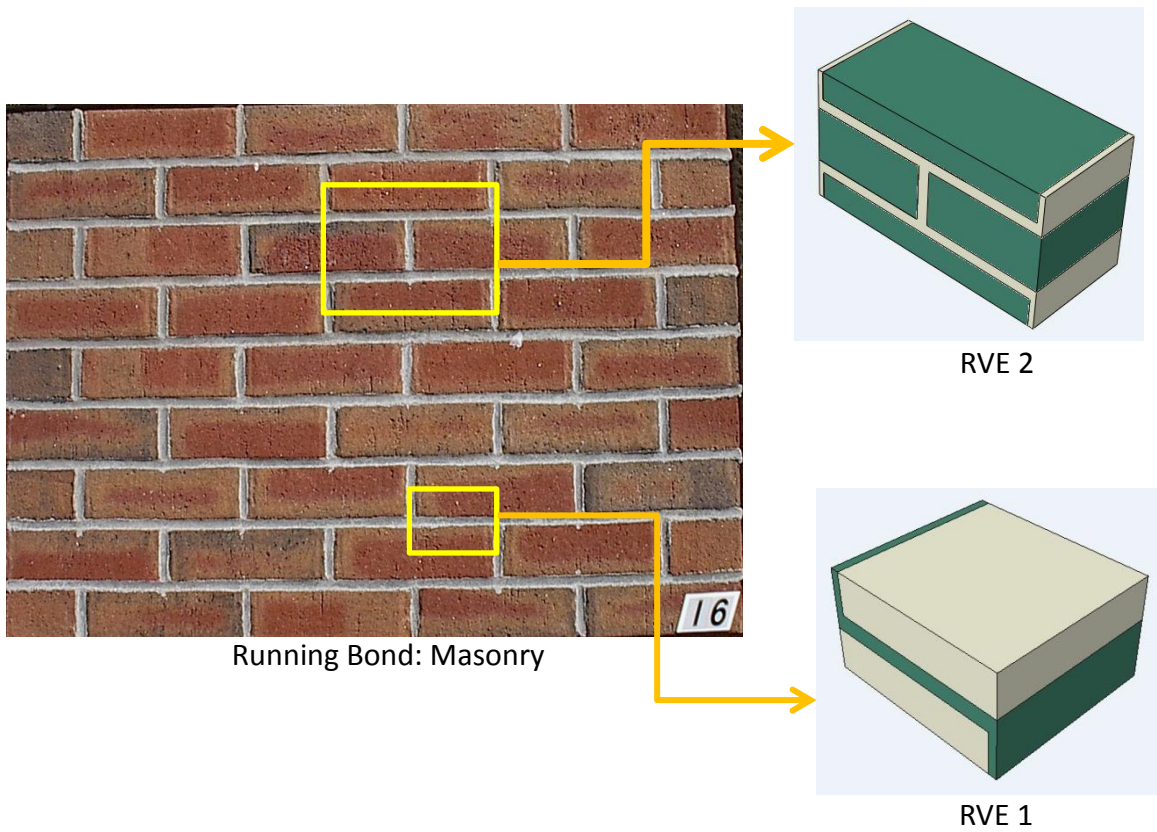


Figure3.1 Definition of masonry axes and of chosen micro mechanical model

Input data considered in the analysis for both RVE's are listed as

Modulus of elasticity of brick = 20Gpa

Modulus of elasticity of mortar = 2Gpa (It will vary for different analysis)

Poisson's ratio of brick and mortar = 0.15

Mortar thickness = 1cm

Brick dimensions: length = 21cm, Height = 5cm, width = 10cm

The figure 3.2 below shows the modal dimensions of the both RVE's

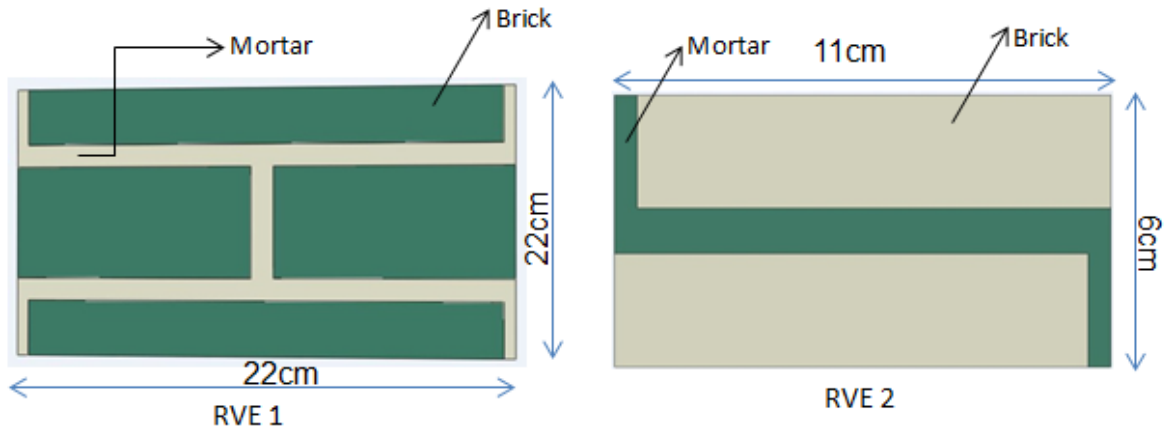


Figure 3.2 Modal dimensions of RVE's

The assumed hypothesis of linear elasticity lets to study the elastic response of the model for a generic loading condition as linear combination of the elastic responses for six elementary loading conditions. In particular, both stress prescribed and strain-prescribed F.E analyses have been carried out. In the following paragraph, the results obtained with the stress-prescribed analysis will be described.

Figure 3.3 below, the finite element model which has been used in the numerical analysis.

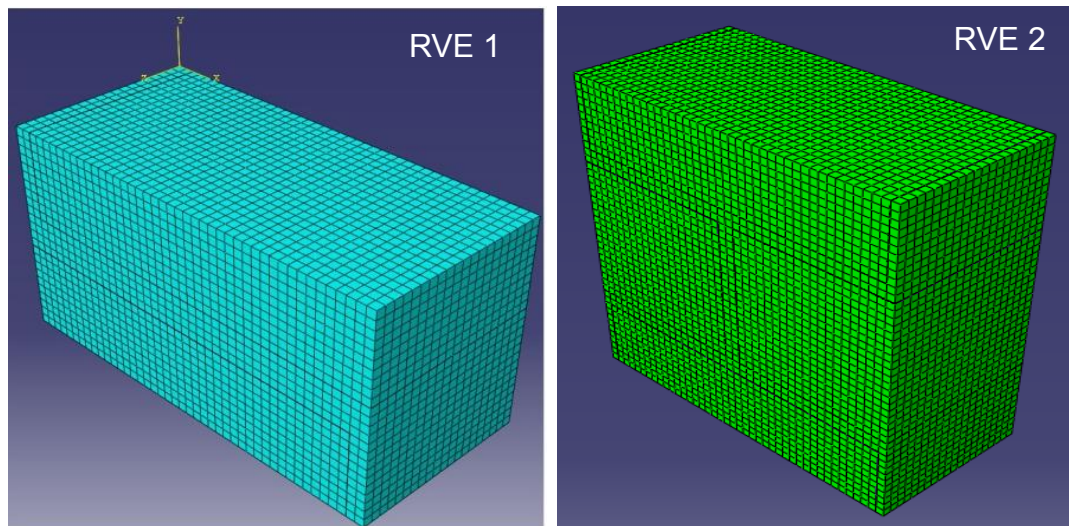


Figure 3.3 Finite element model-mesh

The element type considered was the C3D8R (8 noded linear brick, reduced integration) The mesh was obtained by a process of regular subdivisions of all model lines, by taking into account a mesh size of 0.5 cm.

3.3 Stress-prescribed analysis

In the stress-prescribed analyses, the goal has been to obtain the overall compliance tensor by means of six numerical analyses. Since an orthotropic mechanical behaviour is considered, only nine elastic coefficients will be independent and different from zero.

By using the Voigt notation, so that:

$$\begin{aligned}
 \varepsilon_1 &\rightarrow \varepsilon_{xx} & \varepsilon_4 &\rightarrow 2\varepsilon_{zy} & \sigma_1 &\rightarrow \sigma_{xx} & \sigma_4 &\rightarrow \sigma_{zy} \\
 \varepsilon_2 &\rightarrow \varepsilon_{yy} & \varepsilon_5 &\rightarrow 2\varepsilon_{zx} & \sigma_2 &\rightarrow \sigma_{yy} & \sigma_5 &\rightarrow \sigma_{zx} \\
 \varepsilon_3 &\rightarrow \varepsilon_{zz} & \varepsilon_6 &\rightarrow 2\varepsilon_{xy} & \sigma_3 &\rightarrow \sigma_{zz} & \sigma_6 &\rightarrow \sigma_{xy}
 \end{aligned} \tag{3.1}$$

The stress-strain relation can be written in the following form:

$$\begin{bmatrix} \bar{\varepsilon}_1 \\ \bar{\varepsilon}_2 \\ \bar{\varepsilon}_3 \\ \bar{\varepsilon}_4 \\ \bar{\varepsilon}_5 \\ \bar{\varepsilon}_6 \end{bmatrix} = \begin{bmatrix} \bar{S}_{11} & \bar{S}_{12} & \bar{S}_{13} & 0 & 0 & 0 \\ \bar{S}_{21} & \bar{S}_{22} & \bar{S}_{23} & 0 & 0 & 0 \\ \bar{S}_{31} & \bar{S}_{32} & \bar{S}_{33} & 0 & 0 & 0 \\ 0 & 0 & 0 & \bar{S}_{44} & 0 & 0 \\ 0 & 0 & 0 & 0 & \bar{S}_{55} & 0 \\ 0 & 0 & 0 & 0 & 0 & \bar{S}_{66} \end{bmatrix} \begin{bmatrix} \bar{\sigma}_1 \\ \bar{\sigma}_2 \\ \bar{\sigma}_3 \\ \bar{\sigma}_4 \\ \bar{\sigma}_5 \\ \bar{\sigma}_6 \end{bmatrix} \tag{3.2}$$

Where the superscript $[\bar{\quad}]$ means that the above written equations refer to the average values of the corresponding quantities within the considered RVE. By applying the six loading conditions one at a time, it is possible to obtain the single columns of the compliance tensor, one at a time too, according to the following relation:

$$\bar{S}_{ij} = \frac{\bar{\varepsilon}_i}{\bar{\sigma}_j} \quad i, j = 1, 2, 3, 4, 5, 6 \tag{3.3}$$

3.3.1 Homogenised elastic compliances

When the boundary conditions are applied in terms of uniform stresses on the considered RVE (basic cell), the following relation furnishes the average stress value in the RVE volume

$$\bar{\sigma}_j = \frac{1}{V} \int_V \sigma_j dV = \sigma_j^0 \quad j = 1, 2, 3, 4, 5, 6 \tag{3.4}$$

Where V stands for the volume of the basic cell and σ_j^0 is the generic stress-prescribed component.

The same result is attained if the above shown RVE is considered subjected, for an example, to a unit stress component σ_j^0 , i.e

$$p = \sigma_j^0 = -1 \quad (3.5)$$

Hence, the resulting force F_j on loaded face is obtained by

$$F_j = \sum_{r=1}^m \bar{\sigma}_j^{(r)} A^{(r)} \quad (3.6)$$

Where

m is the number of the elements in which the loaded face is discretized.

$A^{(r)}$ is the area of generic element

$\bar{\sigma}_j^{(r)}$ is the average value of the j -stress component, for the generic element

Since the used mesh size is constant everywhere, all the areas of the elements are equal, too. So, the equation (5) can be rewritten in the following form

$$F_j = A \sum_{r=1}^m \bar{\sigma}_j^{(r)} \rightarrow \sum_{r=1}^m \bar{\sigma}_j^{(r)} = \frac{F_j}{A} \quad (3.7)$$

By dividing both members for the elements number m , it is obtained:

$$\frac{1}{m} \sum_{r=1}^m \bar{\sigma}_j^{(r)} = \frac{F_j}{mA} = \frac{F}{A_{tot}} \rightarrow \hat{\sigma}_j = p = \sigma_j^0 \quad (3.8)$$

Where:

$\hat{\sigma}_j$ = the average value of the j -stress component on the examined loaded face

A_{tot} = the area of such loaded face

The equation (8) remains unaltered if it is multiplied and divided for l ,

Where l is given by:

$$l = \frac{n}{m} \quad (3.9)$$

and with:

n = the number of the elements, equal to 21120(for RVE1), in which the whole RVE has been discretized.

Since such operation yields the average value of the j -stress component within the whole RVE, it is obtained that:

$$\bar{\sigma}_j = p = \sigma_j^0 = -1 \quad (3.10)$$

At this point, it occurs to calculate the volume average value of strain, $\bar{\varepsilon}_i$, obtained as

$$\bar{\varepsilon}_i = \frac{\sum_{r=1}^n \bar{\varepsilon}_i^{(r)}}{n} \quad (3.11)$$

Where

n = the number of elements in which the whole RVE is discretized .

$\bar{\varepsilon}_i^{(r)}$ = the average value of the i -strain component, for the generic element.

3.3.2 Homogenised properties results from RVE's

In the finite element analysis the individual material properties of brick and mortar are considered. Different stiffness ratios between mortar and unit are considered to plot graphs, This has allowed assessing the performance of the model for inelastic behaviour. In fact, non-linear behaviour is associated with (tangent) stiffness degradation and homogenisation of non-linear processes will result in large stiffness differences between the components. In the limit, the ratio between the stiffness of the different components is zero or infinity.

Figure 3.4 and Figure 3.5 shows variation of E_{unit}/E_{mortar} (x-axis) with normalised young's modulus normalised shear modulus and normalised poissons ratio for RVE1 and RVE2.

The material properties of the unit are kept constant, whereas the properties of the mortar are varied. In particular, for the unit, the Young's modulus E_b is 20 GPa and the Poisson's ratio is 0.15. For the mortar, the Young's modulus is varied to yield a ratio E_b/E_m ranging from 1 to 1000 while the mortar Poisson's ratio is kept constant to 0.15 and equal to that one of the unit.

The adopted range of E_b/E_m is very large (up to 1000). Note that the ratio E_b/E_m tends to infinity when softening of the mortar is complete and only the unit remains structurally active.

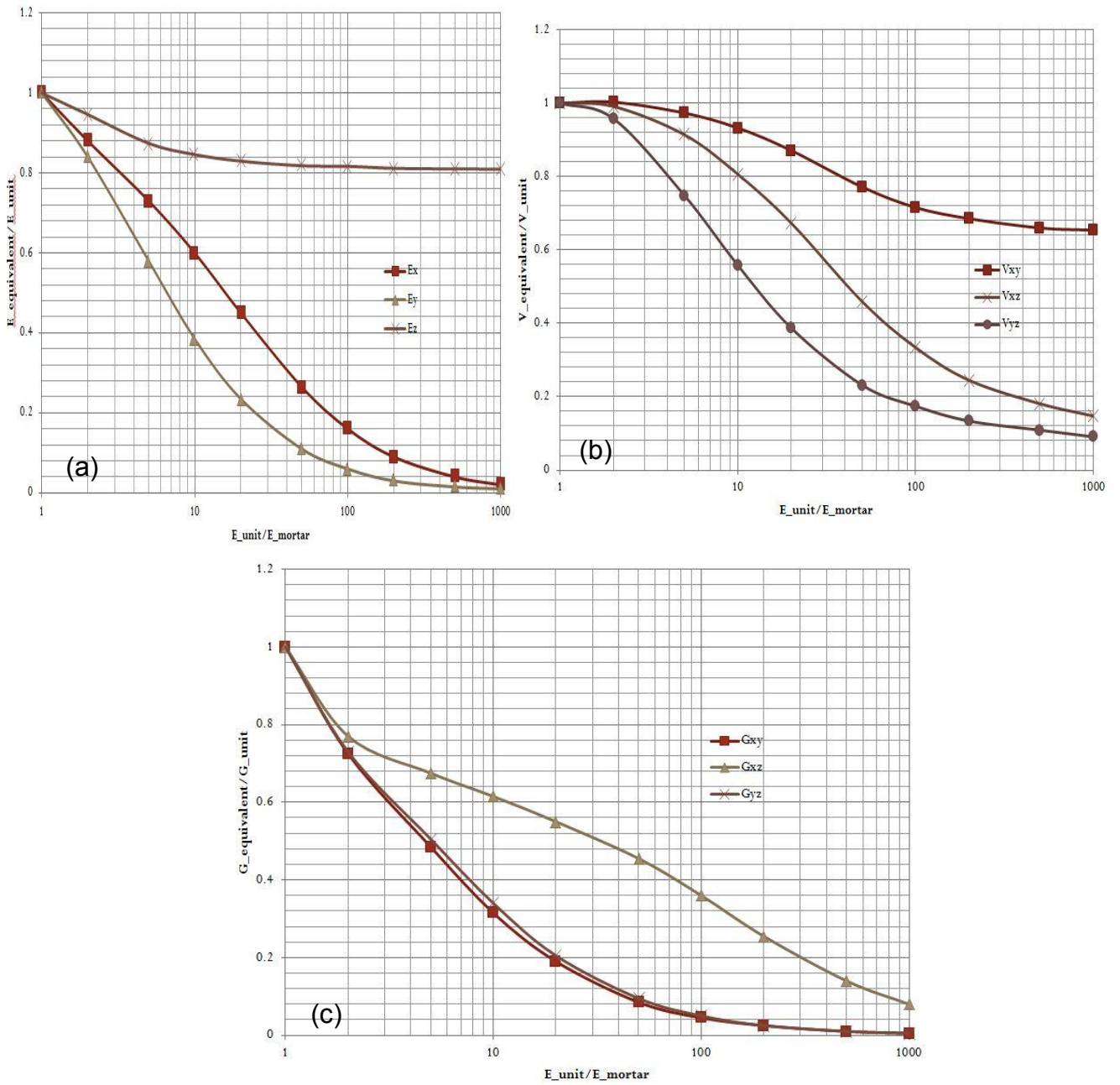


Figure 3.4 FEA results for different stiffness ratios for RVE1: (a) Young's moduli (b) Poisson's ratio and (c) shear moduli.

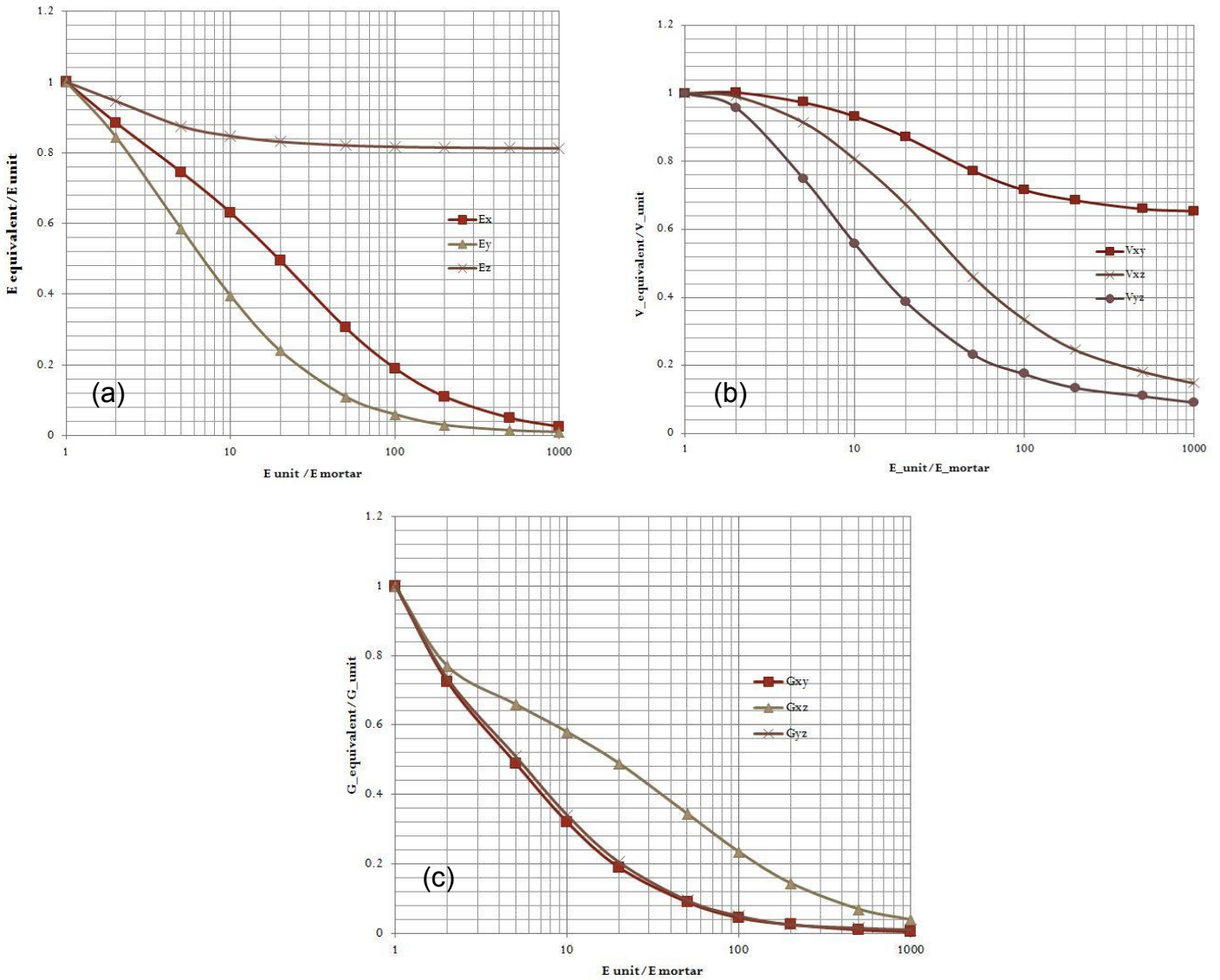


Figure 3.5 FEA results for different stiffness ratios for RVE2: (a) Young's moduli (b) Poisson's ratio and (c) shear moduli.

3.3.3 Effect of mortar modulus

To investigate the effects of mortar moduli on the homogenized equivalent material properties of the unit cell, the material properties of the brick are kept constant whereas the properties of the mortar are varied. Different stiffness ratios of brick to mortar are considered in the analysis. Figure 3.4(a) shows the plots of the ratios of Young's modulus of brick to Young's modulus of mortar (E_b/E_m) ranging from 1 to 1000 vs. the normalized homogenized equivalent Young's moduli and

shear moduli (E_{eq}/E_b and G_{eq}/G_b). Similar trends for equivalent Young's moduli and shear moduli are observed in Figure 3.5. Both (E_{eq}/E_b and G_{eq}/G_b) begin with the value of 1.0 when E_b is equal to E_m , and decrease rapidly at the beginning and then slowly with the increase of the modulus ratio E_b/E_m . E_{zz} is greater than the E_{xx} and E_{yy} , and In-plane shear modulus G_{xy} is also less than the out-of plane shear moduli, G_{yz} and G_{zx} . These observations indicate that the unit cell has higher out-of-plane stiffness than its in-plane stiffness. Because of the out of plane stiffness G_{zx} is more, the in plane Poisson's ratio ν_{xy} is less and we can see it in Figure 3.4(b) graph.

3.4 Strain prescribed analysis

In the strain-prescribed analyses, the goal has been to obtain the overall stiffness tensor by means of six numerical analyses. Since an orthotropic mechanical behaviour is considered, only nine elastic coefficients will be independent and different from zero.

By remembering the Voigt notation, the stress-strain relation can be written in the following form

$$\begin{bmatrix} \bar{\sigma}_{xx} \\ \bar{\sigma}_{yy} \\ \bar{\sigma}_{zz} \\ \bar{\sigma}_{yz} \\ \bar{\sigma}_{zx} \\ \bar{\sigma}_{xy} \end{bmatrix} = \begin{bmatrix} \bar{C}_{11} & \bar{C}_{12} & \bar{C}_{13} & 0 & 0 & 0 \\ \bar{C}_{21} & \bar{C}_{22} & \bar{C}_{23} & 0 & 0 & 0 \\ \bar{C}_{31} & \bar{C}_{32} & \bar{C}_{33} & 0 & 0 & 0 \\ 0 & 0 & 0 & \bar{C}_{44} & 0 & 0 \\ 0 & 0 & 0 & 0 & \bar{C}_{55} & 0 \\ 0 & 0 & 0 & 0 & 0 & \bar{C}_{66} \end{bmatrix} \begin{bmatrix} \bar{\varepsilon}_{xx} \\ \bar{\varepsilon}_{yy} \\ \bar{\varepsilon}_{zz} \\ \bar{\varepsilon}_{yz} \\ \bar{\varepsilon}_{zx} \\ \bar{\varepsilon}_{xy} \end{bmatrix}$$

Where the superscript $[-]$ means that the above written equations refer to the average values of the corresponding quantities within the considered RVE. By applying the six loading conditions one at a time, it is possible to obtain the single columns of the stiffness tensor, one at a time too, according to the following relation

$$\bar{C}_{ij} = \frac{\bar{\sigma}_i}{\bar{\varepsilon}_j} \quad i, j = 1, 2, 3, 4, 5, 6 \quad (3.12)$$

3.4.1 Homogenised elastic stiffness

When the boundary conditions are applied in terms of surface displacements on the considered RVE (basic cell), the following relation furnishes the average strain value in the RVE volume

$$\bar{\varepsilon}_j = \frac{1}{V} \int_V \varepsilon_j dV = \varepsilon_j^0$$

Where V stands for the volume of the basic cell and ε_j^0 is the generic strain component so that:

$$\varepsilon^0 \cdot x = u^0$$

With

u^0 = prescribed surface displacement

More in detail, in order to find the homogenized stiffness tensor, the average strain value within the RVE volume is obtained as

$$\bar{\varepsilon}_j = \varepsilon_j^0 = \sum_{r=1}^n \frac{\bar{\varepsilon}_j^{(r)}}{n}$$

n = the number of elements in which the whole RVE is discretized and equal to 21120 (for RVE1).

$\bar{\varepsilon}_j^{(r)}$ = the average value of the j -strain component, for the generic element.

At this point, it occurs to calculate the average value of stress, $\bar{\sigma}_i$ obtained as

$$\bar{\sigma}_i = \frac{\sum_{r=1}^n \sigma_i^{(r)}}{n} \quad (3.13)$$

Where $\sigma_i^{(r)}$ = the average value of the i -stress component, for the generic element.

3.4.2 Homogenised properties results from RVE's

The material properties of the unit are kept constant, whereas the properties of the mortar are varied. In particular, for the unit, the Young's modulus E_b is 20GPa and the Poisson's ratio is 0.15. For the mortar, the Young's modulus is varied to yield a ratio E_b/E_m ranging from 1 to 1000 while the mortar Poisson's ratio is kept constant to 0.15 and equal to that one of the unit.

Figure 3.6 and Figure 3.7 shows variation of E_{unit}/E_{mortar} (x-axis) with normalised young's modulus normalised shear modulus for RVE1 and RVE2.

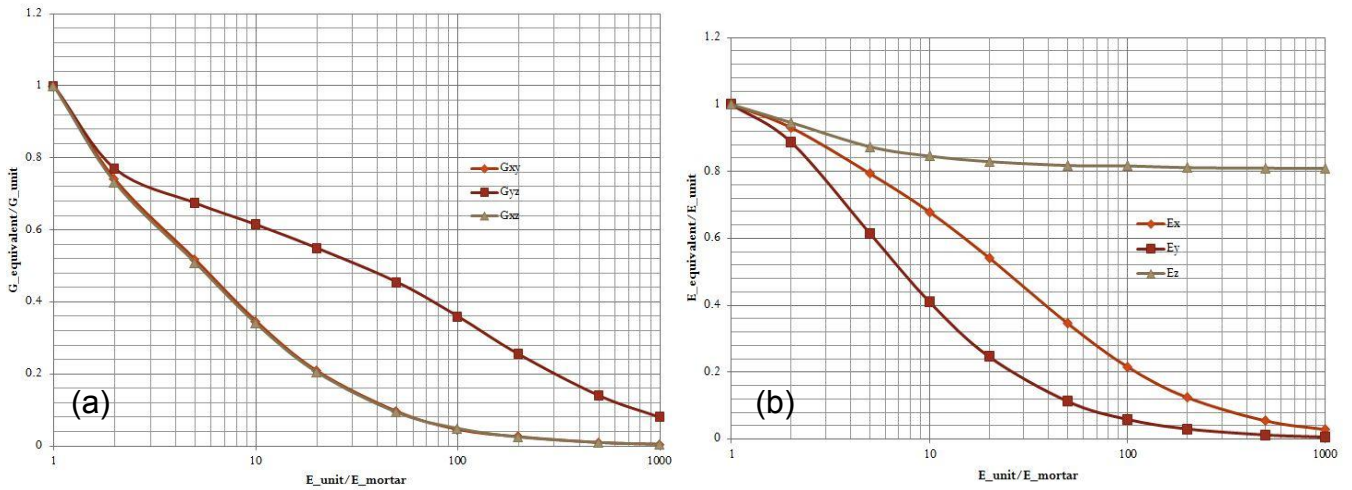


Figure 3.6 FEA results for different stiffness ratios for RVE1: (a) Young's moduli and (b) shear moduli.

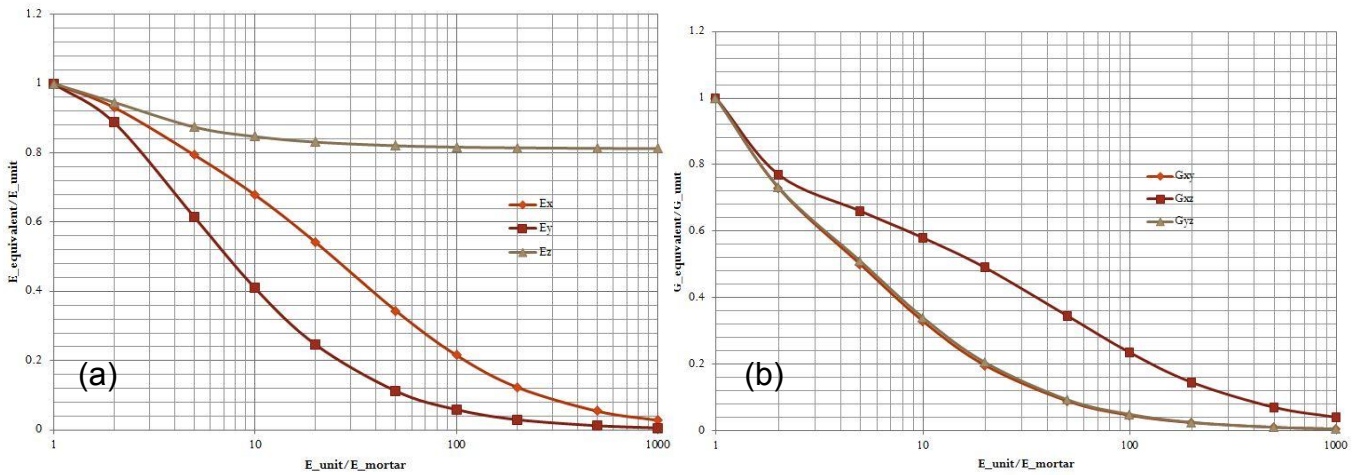


Figure 3.7 FEA results for different stiffness ratios for RVE2: (a) Young's moduli and (b) shear moduli.

3.5 Homogenisation of masonry strengthening by CFRP

The masonry is made of UNI clay bricks, whereas the mortar joint thickness is 10 mm for head joint and 10mm for bed joint in the case of un-strengthened masonry. When the strengthened masonry is considered, the horizontal joint thickness is composed of two mortar layer 4.4 mm thick and one central layer of CFRP material 1.2 mm thick as shown in figure8 below. In fact the CFRP repointing technique reduces the mortar bed joint thickness in the measure of the CFRP thickness. The whole thickness of bed joint is still 10 mm. The assume material properties are: Young's modulus of CFRP

145Mpa, poisons ratio of CFRP 0.2, Young's modulus of brick is 90Gpa and poisons ratio of brick and mortar is 0.15.

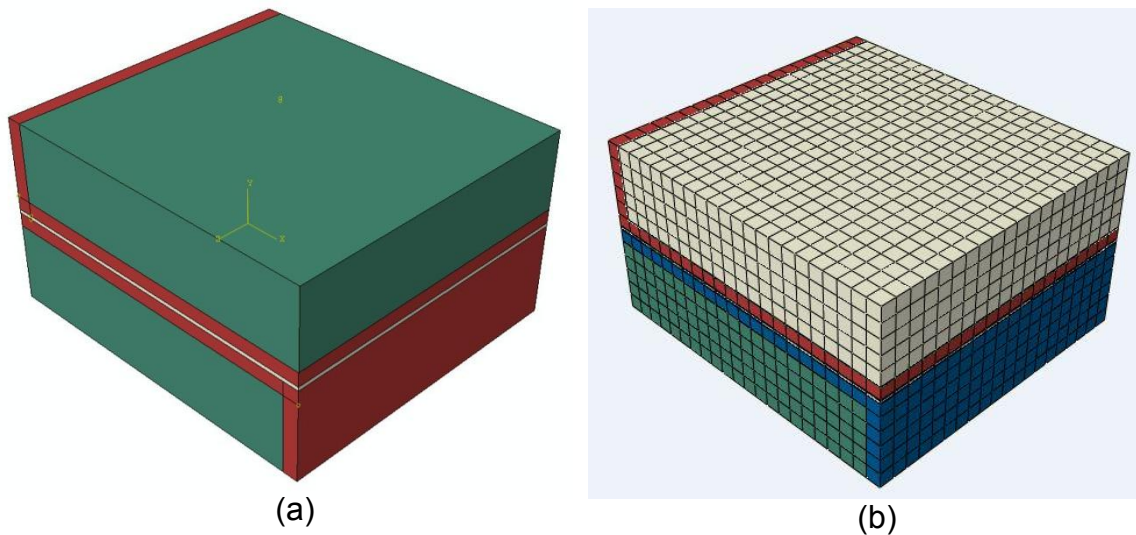


Figure 3.8 (a) FE model of RVE with CFRP (b)FE discretization

The below figures shows that variation of young's modulus and shear modulus for strengthened and unstrengthen masonry

From figure 3.9 and figure 3.10, by using the CFRP the out of plane shear modulus G_{zx} strength is becoming high compared to the other shear modulus values. And young's modulus E_{zz} , E_{xx} also showing high values compared to the E_{yy} modulus for the strengthen and unstrengthen masonries.

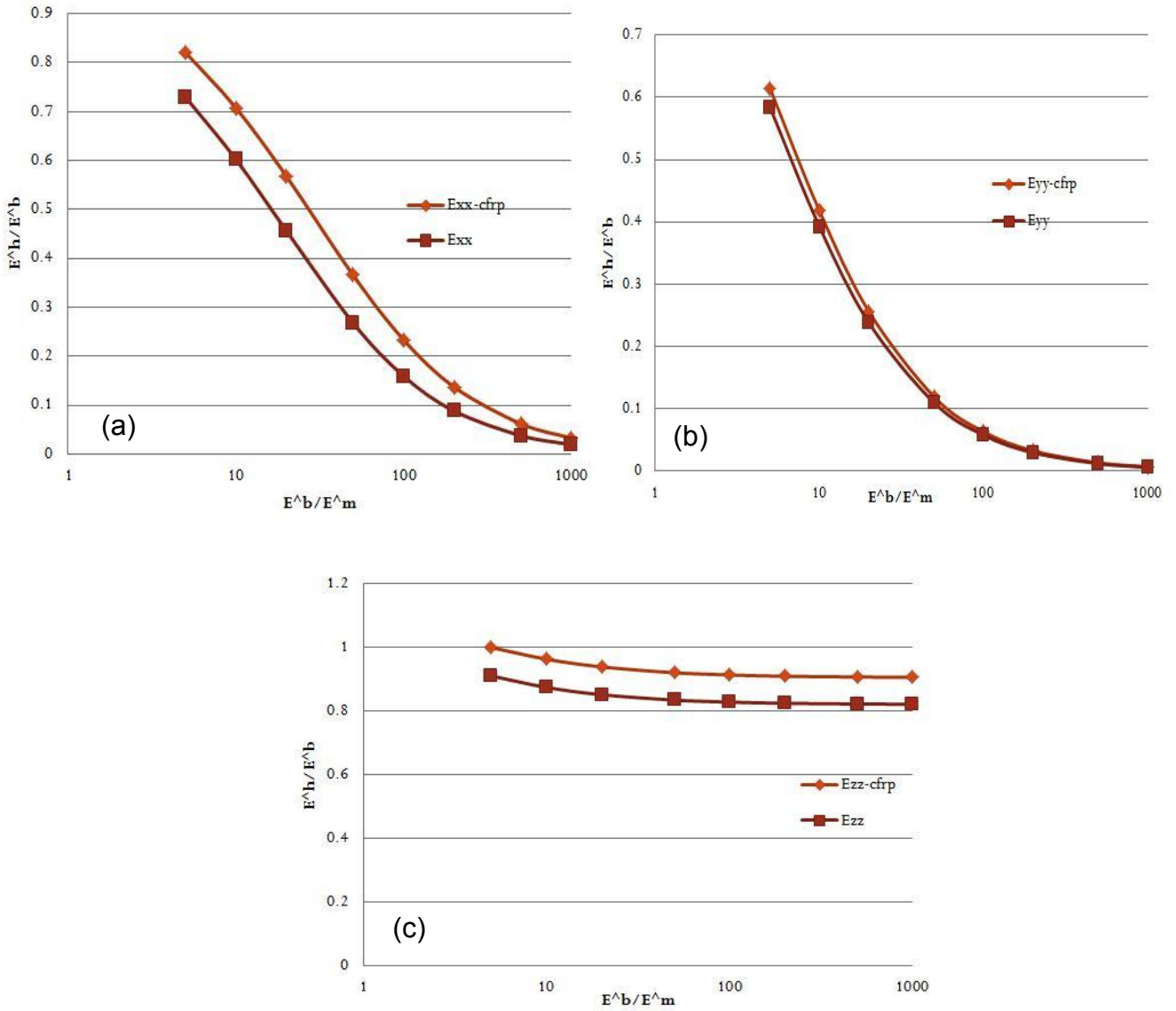


Figure 3.9 FEA results for different stiffness ratios of (a) young's modulus in x direction (b) young's modulus in Y direction (c) young's modulus in Z direction

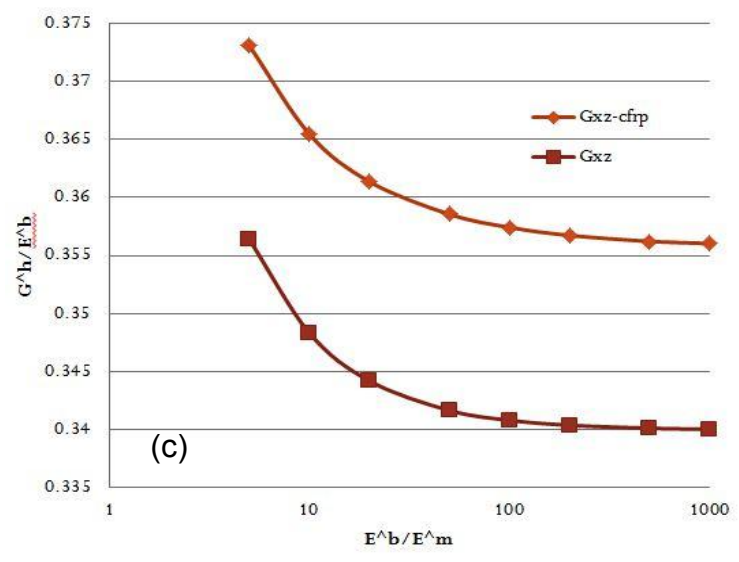
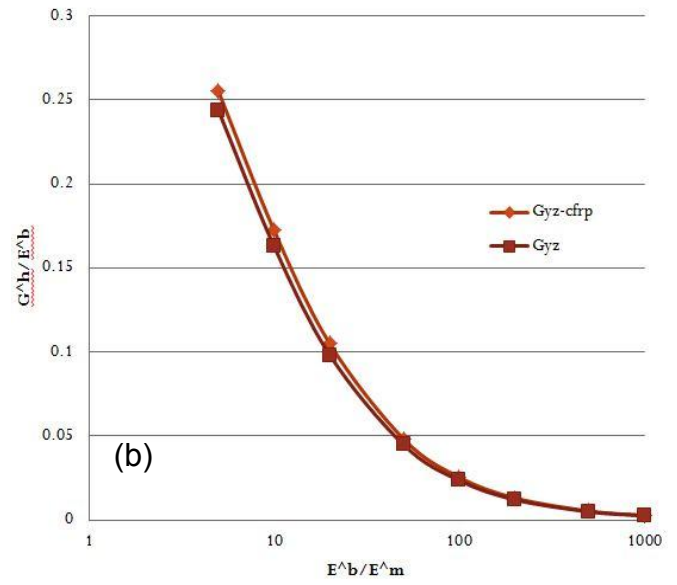
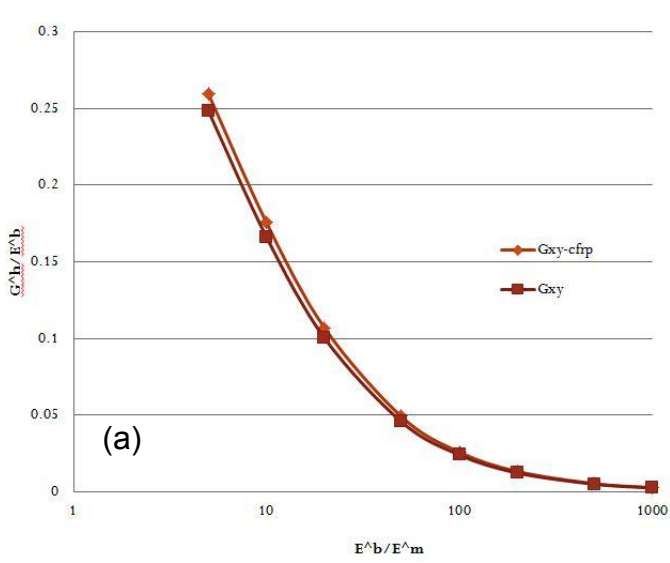


Figure 3.10 FEA results for different stiffness ratios of (a) shear modulus in XY (b) shear modulus in YZ (c) shear modulus in ZX

3.6 Conclusion

In this study, effective properties or homogenised properties of masonry have been found from micromechanics RVE (representative volume element) analysis. Average theorems are used to find the effective properties of masonry. Average stresses and average strains are found from FE analysis, six numerical analysis are carried out to find the stiffness matrix and compliance matrix.

In this work we investigated the effects of mortar moduli on the homogenized equivalent material properties of the unit cell, the material properties of the brick are kept constant whereas the properties of the mortar are varied. Different stiffness ratios of brick to mortar are considered in the analysis and the plots of the ratios of Young's modulus of brick to Young's modulus of mortar (E_b/E_m) ranging from 1 to 1000 vs. the normalized homogenized equivalent Young's moduli and shear moduli (E_{eq}/E_b and G_{eq}/G_b) are made. Both (E_{eq}/E_b and G_{eq}/G_b) begin with the value of 1.0 when E_b is equal to E_m , and decrease rapidly at the beginning and then slowly increase of the modulus ratio E_b/E_m . E_{zz} is greater than the E_{xx} and E_{yy} , and In-plane shear modulus G_{xy} is also less than the out-of plane shear moduli G_{yz} and G_{zx} . These observations indicate that the unit cell has higher out-of-plane stiffness than its in-plane stiffness. Because of the out of plane stiffness G_{zx} is more, the in plane Poisson's ratio ν_{xy} is less.

Plots are also made for strengthen with CFRP and unstrengthen masonry, using the CFRP. The out of plane shear modulus G_{zx} strength is becoming high compared to the other shear modulus values. And young's modulus E_{zz} , E_{xx} also showing high values compared to the E_{yy} modulus for the strengthen and unstrengthen masonries.

Chapter 4

Failure modelling of periodic composites

4.1 Introduction

Masonry can be analysed in different scales such as micro model, meso model and macro model. Masonry is composite material which exhibit distinct directional properties due to mortar joints. In literature the approach run towards micro modelling of individual components of unit or brick and mortar or the macro modelling of masonry. Depending on the level of accuracy and simplicity desired, it is possible to use following modelling strategies:

- Detailed micro modelling- units and mortar in joints are represented by continuum elements whereas the unit mortar interface represented by discontinuous elements;
- Simplified micro modelling- expanded units are represented by continuum elements whereas the behaviour of the mortar joints and unit mortar interface is lumped in discontinuous elements;
- Macro modelling- units, mortar and unit-mortar interface are smeared out in the continuum.

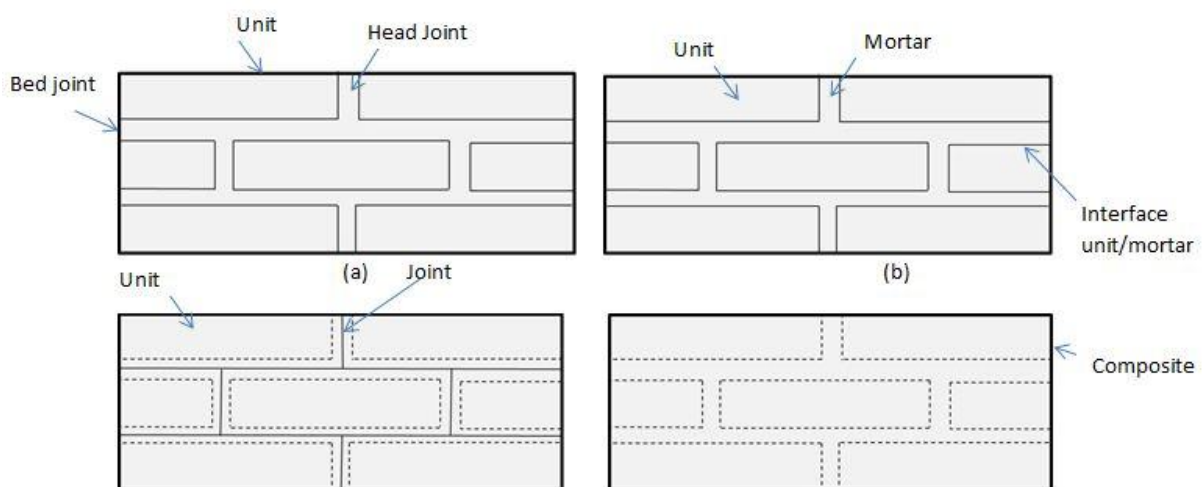


Figure 4.1 Modelling of masonry structures (a) masonry sample; (b) detailed micro modelling; (c) simplified micro-modelling; (d) macro modelling.

In the first modelling, Young's modulus, Poisson's ratio and, optionally, inelastic properties of both unit and mortar are taken into account. The interface represents a potential crack/slip plane with initial dummy stiffness to avoid interpenetration of the continuum. This enables the combined action of unit, mortar and interface to be studied. In the second modelling, each joint, consisting of mortar and the two unit-mortar interfaces, is lumped into an "average" interface while the units are expanded in order to keep the geometry unchanged. Masonry is thus considered as a set of elastic blocks bonded by potential fracture/slip lines at the joints. Accuracy is lost since Poisson's effect of the mortar is not included. The third approach does not make a distinction between individual units and joints but treats masonry as a homogeneous anisotropic continuum. One modelling strategy cannot be preferred over the other because different application fields exist for micro- and macro-models. Micro-modelling studies are necessary to give a better understanding about the local behaviour of masonry structures. This type of modelling applies notably to structural details, but also to modern building systems like those of concrete or calcium-silicate blocks, where window and door openings. Macro-models are applicable when the structure is composed of solid walls with sufficiently large dimensions so that the stresses across or along a macro-length will be essentially uniform. Clearly, macromodeling is more practice oriented due to the reduced time and memory requirements as well as a user-friendly mesh generation. This type of modelling is most valuable when a compromise between accuracy and efficiency is needed.

Accurate micro or macro-modelling of masonry structures requires a thorough experimental description of the material. However, the properties of masonry are influenced by a large number of factors, such as material properties of the units and mortar, arrangement of bed and head joints, anisotropy of units, dimension of units, joint width, quality of workmanship, and degree of curing, environment and age.

4.2 Behaviour of masonry in Different aspects

4.2.1 Softening Behaviour

Softening is a gradual decrease of mechanical resistance under a continuous increase of deformation forced upon a material specimen or structure. It is a salient feature of quasibrittle materials like clay brick, mortar, ceramics, rock or concrete, which fail due to a process of progressive internal crack growth. Such mechanical behaviour is commonly attributed to the heterogeneity of the material, due to the presence of different phases and material defects, like flaws and voids. Even prior to loading, mortar contains micro cracks due to the shrinkage during curing and the presence of the aggregate. The clay brick contains inclusions and micro cracks due to the shrinkage during the burning process. The initial stresses and cracks as well as variations of internal stiffness and strength cause progressive crack growth when the material is subjected to progressive deformation. Initially, the micro cracks are stable which means that they grow only when the load is increased. Around peak load an acceleration of crack formation takes place and the formation of macro cracks starts. The macro cracks are unstable, which means that the load has to decrease to avoid an uncontrolled growth. For shear failure, a softening process is also observed as degradation of the cohesion in Coulomb friction models. For compressive failure, softening behaviour is highly dependent upon the boundary conditions in the experiments and the size of the specimen, [Van Mier (1984) and Vonk (1992)]. Figure 4.2 shows characteristic stress-displacement diagrams for quasi-brittle materials in uniaxial tension and compression. In the present study, it is assumed that the inelastic behaviour both in tension and compression can be described by the integral of the $\sigma - \delta$ diagram. These quantities, denoted respectively as fracture energy G_f and compressive fracture energy G_c , are assumed to be material properties. It is noted that masonry presents other type of failure mechanism, generally identified as mode II, that consists of slip of the unit-mortar interface under shear loading, see Figure 4.3. Again, it is assumed that the inelastic behaviour in shear can be described by the mode II fracture energy G_{IIr} , defined by the integral of the $\tau - \delta$ diagram in the absence of normal confining load. Shear failure is a salient feature of masonry behaviour which must

be incorporated in a micro-modelling strategy. However, for continuum models, this failure cannot be directly included because the unit and mortar geometries are not discretized. Failure is then associated with tension and compression modes in a principal stress space.

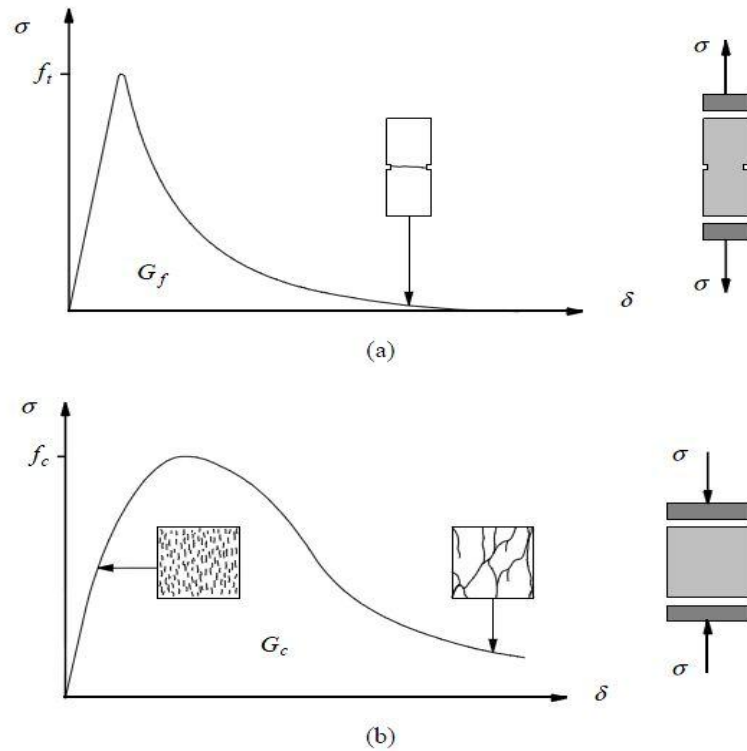


Figure 4.2 Typical behaviour of quasi-brittle materials under uniaxial loading (a) tensile loading (f_t denotes the tensile strength); (b) compressive loading (f_c denotes the compressive strength). [Lourenco 2006]

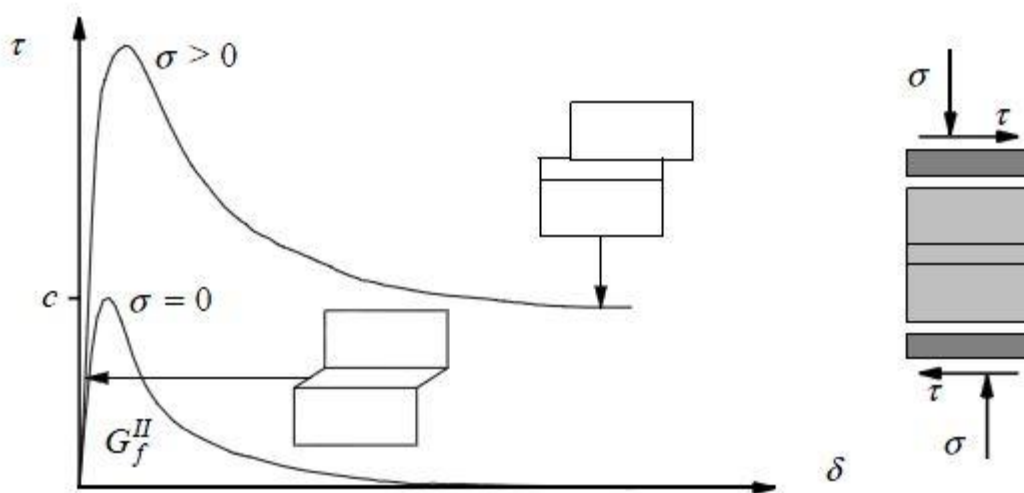


Figure 4.3 Behaviour of masonry under shear (c denotes the cohesion). [Lourenco 2006]

4.2.2 Uniaxial compressive behaviour

The compressive strength of masonry in the direction normal to the bed joints has been traditionally regarded as the sole relevant structural material property, at least until the recent introduction of numerical methods for masonry structures. A test frequently used to obtain this uniaxial compressive strength is the stacked bond prism, it has been accepted by the masonry community that the difference in elastic properties of the unit and mortar is the main for failure. Uniaxial compression of masonry leads to a state of triaxial compression in the mortar and of uniaxial compression and biaxial tension in the unit. Mann and Betzler (1994) observed that, initially, vertical cracks appear in the units along the middle line of the specimen, i.e. continuing a vertical joint. Upon increasing deformation additional cracks appear, normally vertical cracks at the small side of the specimen, that lead to failure by splitting of the prism. Examples of load-displacement diagrams obtained in $500 \times 250 \times 600$ mm prisms of solid soft mud bricks are shown in Figure 4. Increasing strength leads to a more brittle behaviour.

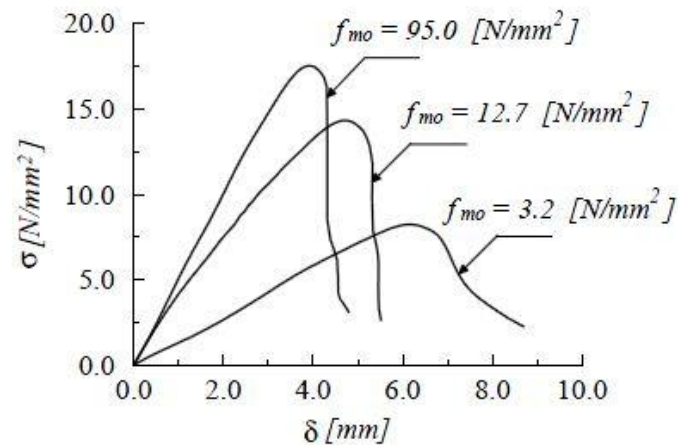


Figure 4.4 Typical experimental stress-displacement diagrams for $500 \times 250 \times 600$ [mm³] prisms of solid soft mud brick, Binda *et al.* (1988). Here, f_{m0} is the mortar compressive strength.

4.2.3 Uniaxial tensile Behaviour

For tensile loading perpendicular to the bed joints, failure is generally caused by failure of the relatively low tensile bond strength between the bed joint and the unit. As a rough approximation,

the masonry tensile strength can be equated to the tensile bond strength between the joint and the unit.

For tensile loading parallel to the bed joints a complete test program was set-up by Backes (1985). The specimen consists of four courses, initially laid down in the usual manner, A special device attached to the specimen turns it 90° in the intended direction of testing shortly before the test time, The load is applied via steel plates attached to the top and bottom of the specimen by special glue. The entire load-displacement diagram is traced upon displacement control.

Two different types of failure are possible, depending on the relative strength of joints and units, see Figure 4.5. In the first type of failure cracks zigzag through head and bed joints. A typical stress-displacement diagram shows some residual plateau upon increasing deformation. The post-peak response of the specimen is governed by the fracture energy of the head joints and the post-peak mode II behaviour of bed joints. In the second type of failure cracks run almost vertically through the units and head joints. A typical stress-displacement diagram shows progressive softening until zero. The post peak response is governed by the fracture energy of the units and head joints.

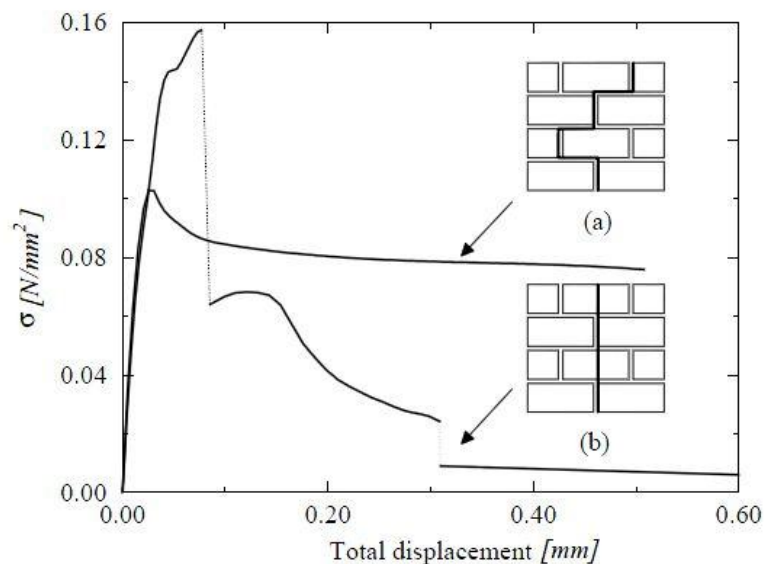


Figure 4.5 Typical experimental stress-displacement diagrams for tension in the direction parallel to the bed joints, Backes (1985): (a) failure occurs with a stepped crack through head and bed joints; (b) failure occurs vertically through head joints and units.

4.3 Damage modelling of masonry

Main focus is to develop a modelling frame work to representing damage behaviour of masonry for macro model and simplified micro model. This involves several aspects of theoretical and practical interest. Important issues include material models, element types, mesh, convergence and boundary conditions. A general conclusion regarding these issues is that the model must be rich to be able to capture the important phenomena, but it should not be more complex than necessary since this would only increase the computer time needed. Abaqus/standard was used for the finite element modelling in this work. This FEM package includes large variety of material models and elements including facilities necessary for this subject.

4.3.1 Constitutive model

(a) For Brick, concrete or quasi brittle materials

In the last decades, many constitutive models which can predict the behaviour of brick, including cracks and crushing have been developed. Two approaches are available in Abaqus to predict the behaviour of concrete or brick: smeared crack and plastic damage models. The plastic damage model was selected for this study since it has higher potential for convergence compared to the smeared crack model.

The concrete plastic damage model assumes that the two main concrete failure mechanisms are cracking and crushing. Crack propagation is modelled by using continuum damage mechanics, stiffness degradation.

The plastic damage model requires the values of elastic modulus, Poisson's ratio, the plastic damage parameters and description of compressive and tensile behaviour. The five plastic damage parameters are the dilation angle, the flow potential eccentricity, the ratio of initial equibiaxial compressive yield stress to initial uniaxial compressive yield stress, the ratio of the second stress invariant on the tensile meridian to that on the compressive meridian and the viscosity parameter that defines viscoplastic regularization. The values of the last four parameters were recommended by the Abaqus documentation for defining concrete material and were set to 0.1, 1.16, 0.66, and 0.0,

respectively. The dilation angle and Poisson's ratio were chosen to be 37° and 0.15, respectively. Another important thing is to represent the stress-strain curve for concrete in an accurate way. For a given brick characteristic compressive strength, the stress-strain curve can be defined beyond the ultimate stress, into the strain-softening regime. The compressive inelastic strain, $\tilde{\varepsilon}_{oc}^{in}$ is defined as the total strain minus the elastic strain, $\tilde{\varepsilon}_{oc}^{in} = \varepsilon_c - \varepsilon_{oc}^{el}$, as illustrated in figure 4.6

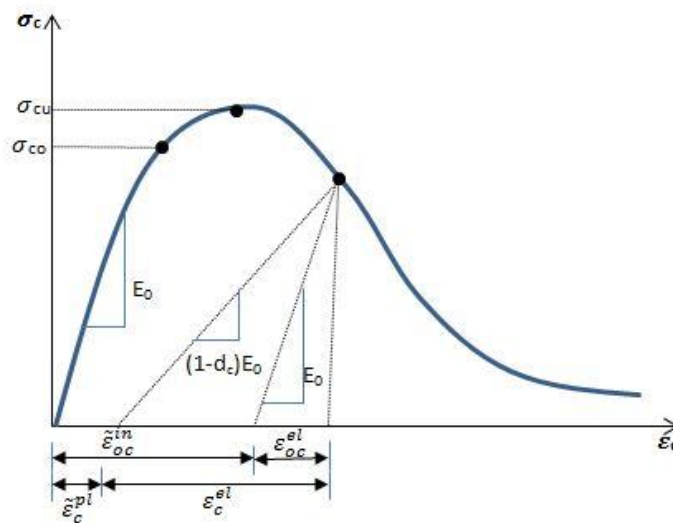


Figure 4.6 Response of concrete to uniaxial loading in compression

The concrete behaviour in tension was modelled using a linear elastic approach until cracking is initiated at tensile strength. After crack initiation, the softening will start. The post-failure behaviour for direct straining is modelled with tension stiffening, which permits to define the strain-softening behaviour for cracked concrete. Tension stiffening is required in the concrete damage plasticity model. It is possible to specify tension stiffening by means of a post-failure stress-strain relation or by applying a fracture energy cracking criterion.

The degradation of the elastic stiffness is characterized by two damage variables, d_t and d_c , which are assumed to be functions of the plastic strains. The damage variables can take values from zero, representing the undamaged material, to one, which represents total loss of strength. Linear relationship between the damage variable and stress was assumed.

(b) Mechanical behaviour

The model is a continuum, plasticity-based, damage model for concrete. It assumes that the main two failure mechanisms are tensile cracking and compressive crushing of the concrete material. The evolution of the yield (or failure) surface is controlled by two hardening variables, $\tilde{\varepsilon}_t^{pl}$ and $\tilde{\varepsilon}_c^{pl}$, linked to failure mechanisms under tension and compression loading, respectively. We refer to $\tilde{\varepsilon}_t^{pl}$ and $\tilde{\varepsilon}_c^{pl}$ as tensile and compressive equivalent plastic strains, respectively. The following sections discuss the main assumptions about the mechanical behaviour of concrete.

Uniaxial Tension and compressive behaviour:

The model assumes that the uniaxial tensile and compressive response of concrete is characterized by damaged plasticity, as shown in Figure 4.7

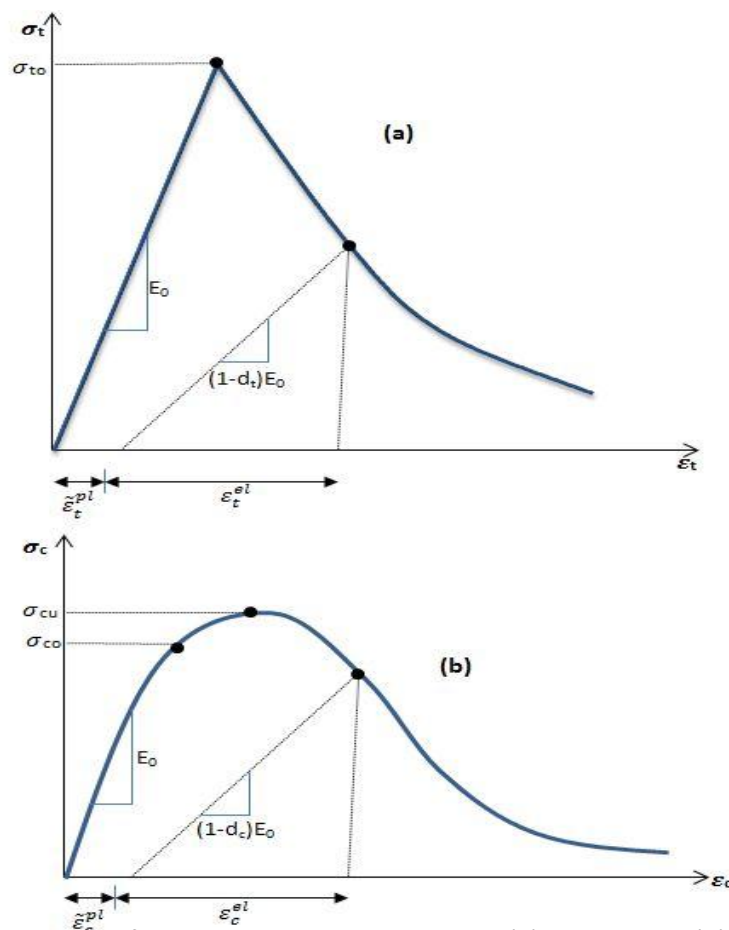


Figure 4.7 Response of concrete to uniaxial loading in (a) tension and (b) compression Under uniaxial tension the stress-strain response follows a linear elastic relationship until

the value of the failure stress, σ_{t0} is reached. The failure stress corresponds to the onset of micro-cracking in the concrete material. Beyond the failure stress the formation of micro-cracks is represented macroscopically with a softening stress-strain response, which induces strain localization in the concrete structure. Under uniaxial compression the response is linear until the value of initial yield, σ_{c0} . In the plastic regime the response is typically characterized by stress hardening followed by strain softening beyond the ultimate stress, σ_{cu} . This representation, although somewhat simplified, captures the main features of the response of concrete.

It is assumed that the uniaxial stress-strain curves can be converted into stress versus plastic-strain curves. (This conversion is performed automatically by Abaqus from the user-provided stress versus “inelastic” strain data, as explained below.) Thus,

$$\sigma_t = \sigma_t(\tilde{\varepsilon}_t^{pl}, \dot{\tilde{\varepsilon}}_t^{pl}, \theta, f_i),$$

$$\sigma_c = \sigma_c(\tilde{\varepsilon}_c^{pl}, \dot{\tilde{\varepsilon}}_c^{pl}, \theta, f_i),$$

Where the subscripts t and c refer to tension and compression, respectively; $\tilde{\varepsilon}_t^{pl}$ and $\tilde{\varepsilon}_c^{pl}$ are the equivalent plastic strains, $\dot{\tilde{\varepsilon}}_t^{pl}$ and $\dot{\tilde{\varepsilon}}_c^{pl}$ are the equivalent plastic strain rates, θ is the temperature, and are f_i other predefined field variables.

When the concrete specimen is unloaded from any point on the strain softening branch of the stress-strain curves, the unloading response is weakened: the elastic stiffness of the material appears to be damaged (or degraded). The degradation of the elastic stiffness is characterized by two damage variables, d_t and d_c , which are assumed to be functions of the plastic strains, temperature, and field variables:

$$d_t = d_t(\tilde{\varepsilon}_t^{pl}, \theta, f_i); \quad 0 \leq d_t \leq 1$$

$$d_c = d_c(\tilde{\varepsilon}_c^{pl}, \theta, f_i); \quad 0 \leq d_c \leq 1$$

The damage variables can take values from zero, representing the undamaged material, to one, which represents total loss of strength.

If E_0 is the initial (undamaged) elastic stiffness of the material, the stress-strain relations under uniaxial tension and compression loading are, respectively:

$$\sigma_t = (1 - d_t)E_0(\varepsilon_t - \tilde{\varepsilon}_t^{pl}),$$

$$\sigma_c = (1 - d_c)E_0(\varepsilon_c - \tilde{\varepsilon}_c^{pl}).$$

We define the “effective” tensile and compressive cohesion stresses as

$$\bar{\sigma}_t = \frac{\sigma_t}{(1 - d_t)} = E_0(\varepsilon_t - \tilde{\varepsilon}_t^{pl}),$$

$$\bar{\sigma}_c = \frac{\sigma_c}{(1 - d_c)} = E_0(\varepsilon_c - \tilde{\varepsilon}_c^{pl}).$$

The effective cohesion stresses determine the size of the yield (or failure) surface.

$$\tilde{\varepsilon}_t^{pl} = \tilde{\varepsilon}_t^{ck} - \frac{d_t}{(1-d_t)} \frac{\sigma_t}{E_0} \quad (4.1)$$

$$\tilde{\varepsilon}_c^{pl} = \tilde{\varepsilon}_c^{in} - \frac{d_c}{(1-d_c)} \frac{\sigma_c}{E_0} \quad (4.2)$$

4.4 Failure modelling of masonry under lateral displacements

Masonry wall was modelled by individual properties of brick and mortar, modelling and post processing was completed in Abaqus 6.9. Steel beam is attached on the top of the wall to apply lateral displacements uniformly. The created model of masonry and its FE discretization is shown in below figure 4.8.

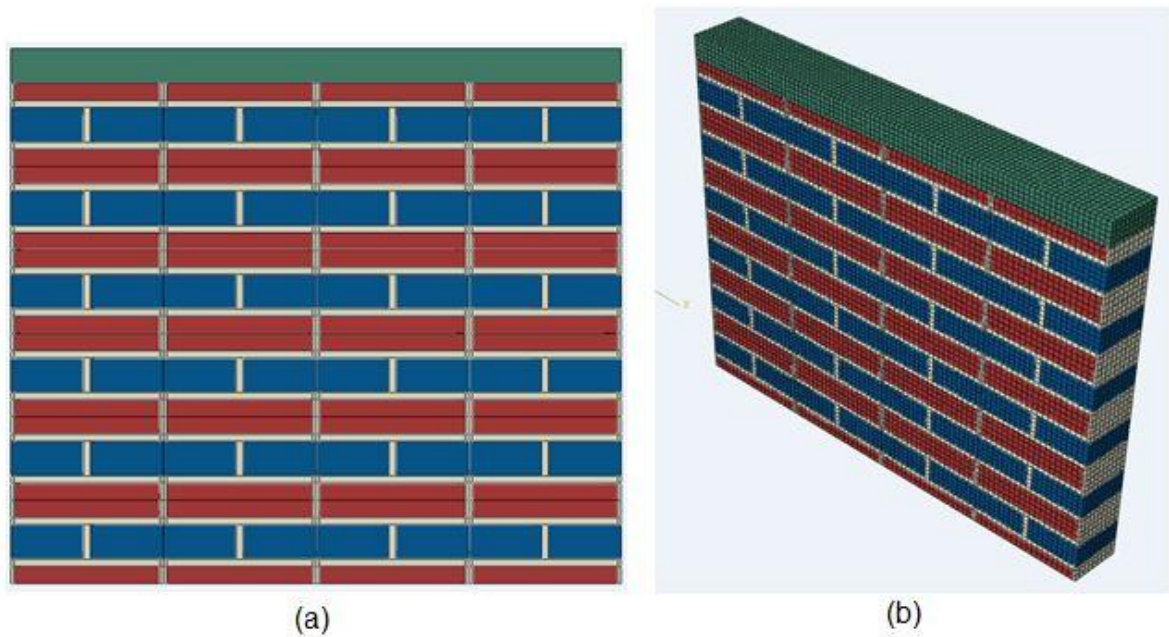


Figure 4.8(a) masonry wall model (b) FE discretization of masonry

Here C3D8R (8 noded linear brick, reduced integration) element is used for analysis and 21*5*10 brick size is used, individual linear isotropic material properties are used and Concrete Damage Plasticity model (CDP) is used along with the isotropic properties. For steel beam elastic perfectly plastic material is assumed.

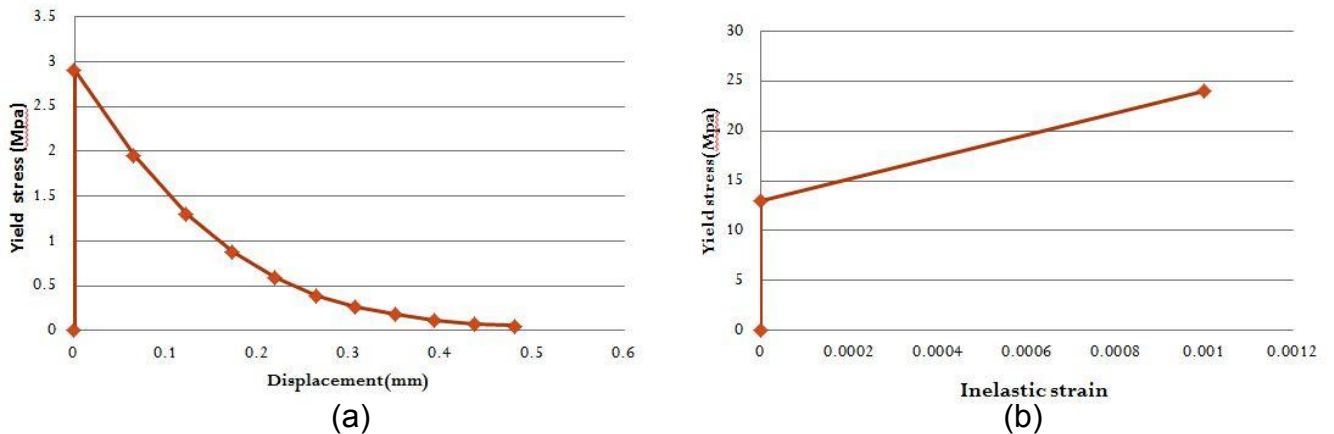
Following are material parameters used in CDP model and figure 4.9 shows the induced compressive and tensile behaviour of masonry.

Dilation angle = $38(\text{For brick})/4$ for mortar

Flow potential eccentricity=0.1

Ratio of initial equibiaxial compressive yield stress to Initial uniaxial compressive yield stress = 1.16

ratio of the second stress invariant =0.66, Viscosity parameter = 0



Bottom face of masonry is fixed and 0.7Mpa pressure is applied on the top face of the steel beam as shown in Figure 4.8, 3mm displacement is applied on the side face of the steel beam so that it displacement was consistently applied on top of wall. The positive equivalent plastic strain gives the damage on the wall as shown in the figure4.10 (a) and figure 4.10(b) horizontal load vs. displacement of the masonry wall. Horizontal tension cracks developed at the bottom and top of the wall at an early loading stage but, ultimately, a diagonal stepped cracks leads to collapse, simultaneously with cracks in bricks and crushing of compressed toes.

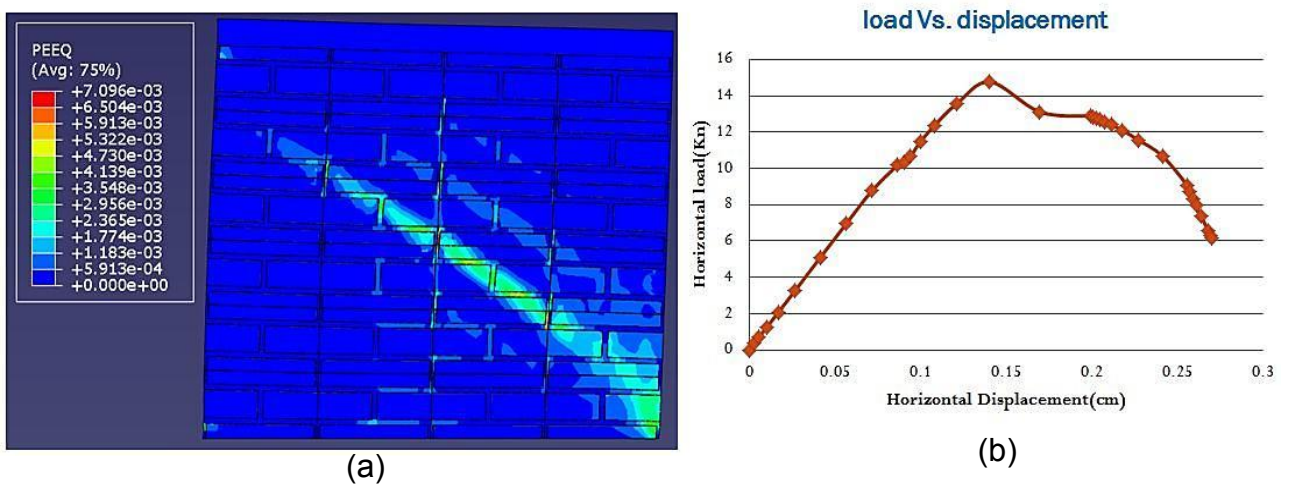


Figure 4.10 (a) damage distribution of masonry wall (b) load vs. displacement graph for masonry

4.5 Multi scale failure theory for composite laminate

Due to the complex structure of composite laminates, consisting of plies made of anisotropic fibres embedded in a polymeric resin, there are a number of complex failure modes, rendering the characterisation very difficult. For instance, a unidirectional laminate subjected to compressive loading may fail by fibre breakage, fibre micro buckling, or transverse delamination. In this regard, research has been devoted to developing predictive failure theories [16]. Early failure theories, such as Tsai-wu theory, treated the lamina as basic building block. Consequently, a large number of mechanical properties are required to determine the coefficients of empirical failure models. Because a ply consists of two phases (fibres and resin) and can fail in several modes, the laminate properties are strongly dependent on stacking sequence, thickness, and operating temperature. Furthermore, it is extremely difficult to extend the conventional laminate failure theories to account for time-dependent failure mechanisms, such as creep and exposure to hot or wet environment.

Recognising the limitations of the conventional laminate failure theories, the researchers have attempted to develop failure criteria that separately model the failure modes of the matrix and the fibres, including the Hashin criterion [19] and Rotem criterion. Both these models use the average stresses in the fibre phase and the matrix phase in determining the onset of initial failure. Stiffness degradation is then required to simulate the fibre-bridging effect in cross-ply laminate. Instead of average stresses as in the Hashin and Rotem criteria multi-continuum theory (MCT)[19] phase averaged stresses, which takes into account the stress amplification effect due to fibre reinforcement in lamina.

4.6 Multi-continuum failure criteria

One common feature between the multi-continuum theory and the strain invariant failure theory is the use of micro-mechanics in determining the stresses within a lamina or ply, which is modelled by a periodic fibre and matrix structure, either of diamond pattern or hexagonal pattern, in this study I consider diamond pattern and the below figure 4.11 is showing diamond configuration RVE which is

modelled in Ansys and its FE discretization. The failure of a fibre-composite material lamina will occur either in the fibres or in matrix, fibre will fail due to shear distortion mode and matrix will fail either due to dilation mode or shear distortion mode.

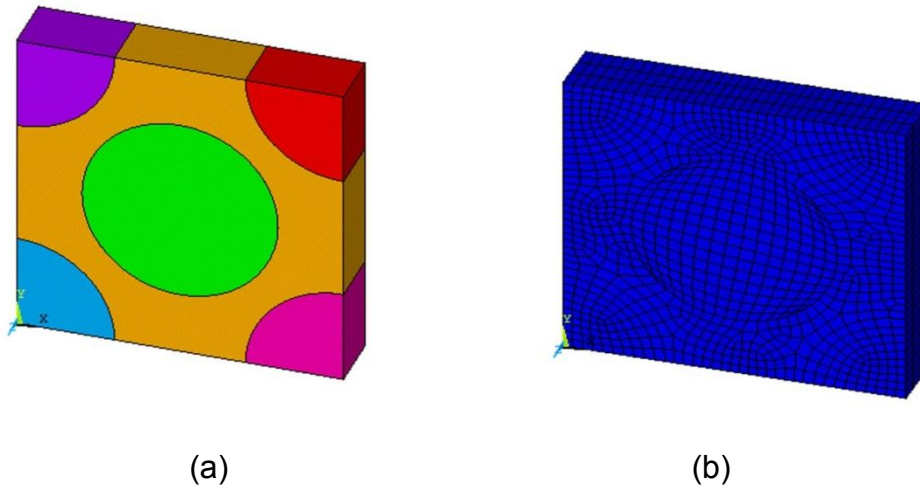


Figure 4.11 Three-dimensional unit cell for reinforced composite (a) diamond configuration RVE (b) FE discretization of RVE

Assumptions for MCT:

- Linear elastic behavior of fiber
- Nonlinear elastic behavior of matrix
- Debonding is not considered here
- Matrix fails either under dilation mode or shear mode
- Pressure sensitivity of matrix is considered
- Fiber failed due to shear distortion or micro buckling.

4.6.1 Fibre failure

The current constituent level failure criteria are based on revised failure criteria originally proposed by Mays [11]. Simple quadratic stress-based failure criteria for fibre is expressed as

$$\pm A_{1f} I_{1f}^2 + A_{4f} I_{4f} = 1, \quad (4.3)$$

Where

$$A_{1f} = \frac{1}{S_{11f}^2},$$

$$A_{4f} = \frac{1}{S_{12f}^2}$$

S_{11f}, S_{12f} are the strength along respective directions

4.6.2 Matrix failure

Simple quadratic stress-based failure criteria for matrix is expressed as

$$\pm A_{1m} I_{1m}^2 - \pm A_{2m} I_{2m}^2 + A_{3m} I_{3m} + A_{4m} I_{4m} - \pm A_{5m} I_{1m} I_{2m} = 1, \quad (4.4)$$

Where

$$A_{2m} = \frac{1}{(S_{22m} + {}^{-22}S_{33m})} \left(1 - \frac{{}^{-}S_{22m} + {}^{-22}S_{33m}}{2S_{23m}^2} \right),$$

$$A_{3m} = \frac{1}{S_{22m}^2 + S_{33m}^2},$$

$$A_{4m} = \frac{1}{S_{12m}^2}$$

And

$$I_1 = \sigma_{11},$$

$$I_2 = \sigma_{22} + \sigma_{33},$$

$$I_3 = \sigma_{22}^2 + \sigma_{33}^2 + 2\sigma_{23}^2,$$

$$I_4 = \sigma_{12}^2 + \sigma_{13}^2,$$

$\pm S_{22m}, \pm S_{33m}, S_{12m}$ are strength along respective directions

In Equation 4.3 and 4.4, the $I_{i\beta}$ terms denote transversely isotropic stress invariants for each constituent, $\beta = f$ for fiber, $\beta = m$ for matrix. The coefficients A_{if} and A_{jm} , leading the invariants, are constituent failure parameters, generally derived from experimentally determined composite ultimate strength data through correlation with the MCT decomposition. The \pm signs in these

equations indicate a dependence of the parameter on tensile versus compressive stress. Details on the computation of these parameters for the analyses presented here-in may be found in Kenik [117]. With the exception of a single parameter, A_{5m} all values of A_{if} and A_{jm} may be determined from a standard set of uniaxial test data. Moreover, parameter A_{5m} may be determined from unidirectional composite biaxial test data ($\sigma_{11} - \sigma_{22}$). In the absence of biaxial data, a reasonable approximation of A_{5m} may be obtained based on the orthotropic failure criteria of Hill [18].

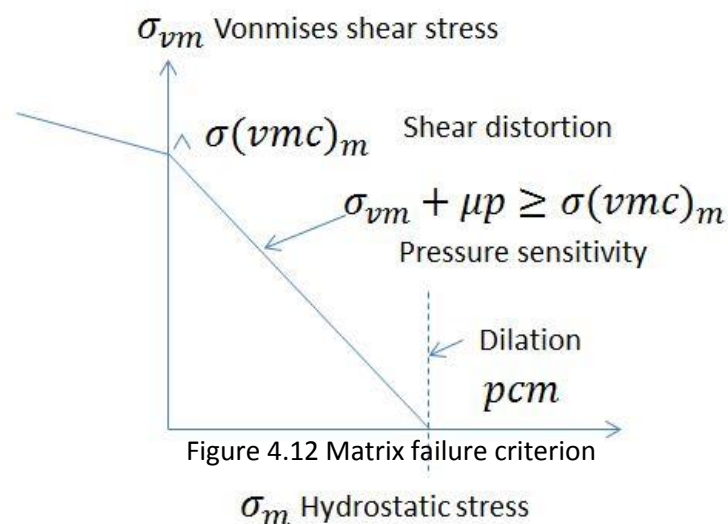
Alternative form for pressure sensitivity

To account for pressure sensitivity of polymeric matrix in the shear distortion failure mode, the modified von Mises yield criterion will be adopted [10] (as illustrated in figure)

$$\sigma_{vm} + \mu p \geq \sigma_{vmc}^m$$

Where σ_{vmc}^m denotes the critical von Mises stress for matrix, μ the pressure sensitivity of the matrix.

To determine the stresses in the fibre and in the matrix, a two-step analysis is required. Firstly the stresses for lamina determined by using laminate theory. Then a micromechanics analysis is performed by using the finite element method to solve for the fibre and matrix stresses where the strains determined in the first step serve as the boundary conditions.



4.7 Laminate analysis

Since the loading axes and the lamina material principle axes do not typically coincide, so the lamina stresses must be transformed from loading axis to the material axis directions. The transformed stress matrix $\bar{\sigma}$ of ply is rotated by an angle θ of and is given as

$$[\bar{\sigma}] = [T]^T [\sigma] [T] \quad (4.5)$$

Where $[T]$ is the transformation matrix expressed as

$$[T] = \begin{bmatrix} m^2 & n^2 & mn \\ n^2 & m^2 & -mn \\ -2mn & 2mn & m^2 - n^2 \end{bmatrix}; \quad m = \cos \theta \quad \& \quad n = \sin \theta \quad \text{And}$$

$$[\sigma] = \begin{bmatrix} \sigma_{11} & \sigma_{12} & \sigma_{13} \\ \sigma_{21} & \sigma_{22} & \sigma_{23} \\ \sigma_{31} & \sigma_{32} & \sigma_{33} \end{bmatrix}$$

4.8 Micromechanics solutions

For either of the unit cells shown in figure 4.3, there is a substantial non uniformity in the matrix stress, due to the disparity in stiffness. An example is shown in figure 4.13 which depicts the stress distribution due to an applied stress. The maximum fibre stresses and the $\{\sigma_f\}$ maximum matrix stresses $\{\sigma_m\}$ are related to the ply stresses,

$$\{\sigma_m\} = [A_m] \{\sigma\}_{12}$$

$$\{\sigma_f\} = [A_f] \{\sigma\}_{12}$$

Where matrices $[A_m]$ and $[A_f]$ denote the amplification factors, which can be determined by using the finite element method for a given fibre volume fraction and fibre-matrix combination. The micromechanics model is based on an assumed periodic fibre configuration within the lamina's matrix, either in the form of repeating diamond or hexagonal unit cell shown in figure 4.11. To enforce compatibility of the unit cell boundaries, i.e., boundaries remains plane after deformation,

the nodes along the unit cell boundaries is constrained to undergo the same displacement normal to the boundary.

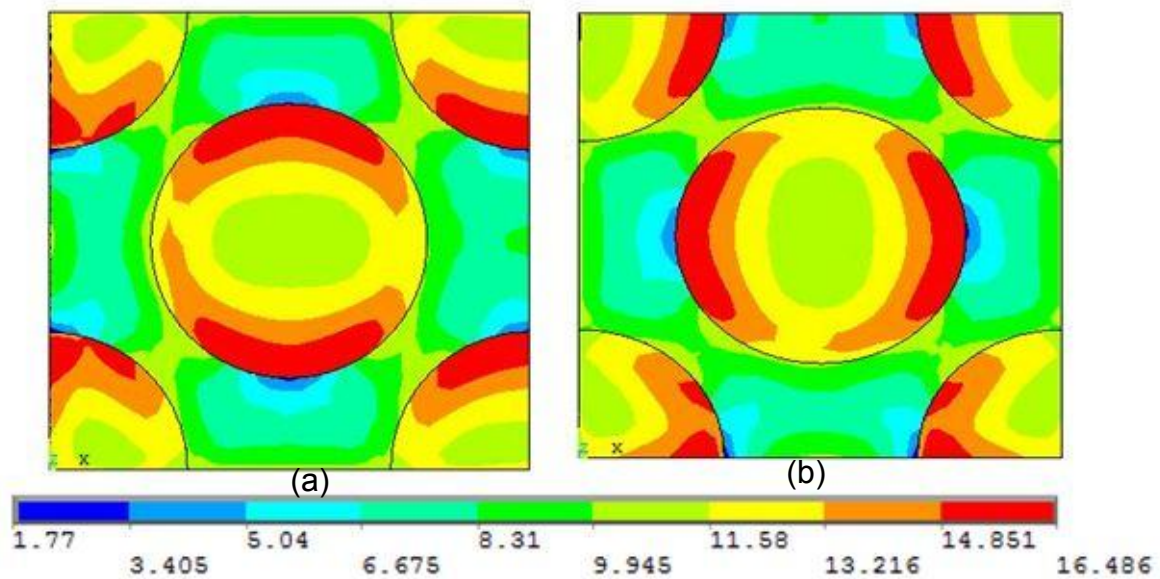


Figure 4.13 stress distribution in a carbon/epoxy lamina subjected to a unit applied stresses: (a) σ_{xx} and (b) σ_{yy}

4.9 Phase degradation approach

The failure criteria presented in section are valid only for a lamina. For a composite laminate, the failure of a single lamina may not cause the rupture of the laminate, as the failed lamina may be bridged by other plies. Therefore the ultimate failure strength of a laminate may be significantly higher than the initial failure strength of the most highly stressed lamina in laminate. One efficient approach to account for this damage progression through the laminate is to adopt a phase degradation approach in which the fibre stiffness or the matrix stiffness is reduced in accordance with failure modes; longitudinal fibre stiffness is reduced to zero should fibre fracture occur, whereas matrix shear stiffness is reduced if the matrix failure is detected. Ply stiffness is recalculated by using the modified rule of mixture [15]; details will be presented in the following. As the damage progression through the laminate, eventual failure will occur due to either excessive deformation or insufficient load carrying capacity (i.e., failure have completely progressed through all the laminae).

In the case of fibre failure, resulting from either shear distortion or compressional micro buckling, the longitudinal stiffness of the fibre phase is assumed to degrade to zero. In other words, the effective longitudinal stiffness of the fibre phase is assumed to degrade to zero. In other words, the effective longitudinal stiffness can be expressed as

$$E_{f1}^* = \begin{cases} E_{f1} & \varepsilon_{vm}^{(f)} < \varepsilon_c^{(f)} \text{ or } \sigma_1^{(f)} > \sigma_c^{(f)} \\ 0 & \text{otherwise} \end{cases} \quad (4.6)$$

For the matrix, it is necessary to account for the relatively high degree of plastic deformation. In this case, the effective shear modulus is taken to be equal to the secant shear stiffness before the shear strain reaches a critical value, as described by the following relations,

$$G_m^* = \begin{cases} G_m & \sigma_{vm} + \mu p < \sigma_c^{(m)} \\ \tau_{oct}^m / \gamma_{oct}^{(m)} & \sigma_{vm} + \mu p \geq \sigma_c^{(m)} \text{ and } \gamma_{oct}^{(m)} \leq \gamma_c^{(m)} \\ 0 & \text{otherwise} \end{cases} \quad (4.7)$$

Where τ_{oct}^m and $\gamma_{oct}^{(m)}$ denote the octahedral shear stress and shear strain in the matrix. The value of $\gamma_c^{(m)}$ for a polymeric matrix material can be readily obtained through the in-plane shear stress or strain data. As an example, for the four fibre or epoxy laminates employed in the world-wide failure exercise study.

Now the ply properties can be expressed in terms of the fibre and matrix properties via the modified rule of mixture [15],

$$E_{11}^* = V_f E_{f1}^* + (1 - V_f) E_m^*$$

$$E_{22}^* = E_{33}^* = 2(1 + \nu_m) G_m^* \frac{1 + \xi_1 \eta_1 V_f}{1 - \eta_1 V_f}, \text{ with } \eta_1 = \frac{E_{f2}/E_m - 1}{E_{f2}/E_m + \xi_1}$$

$$G_{12}^* = G_m^* \frac{1 + \xi_2 \eta_2 V_f}{1 - \eta_2 V_f}, \text{ with } \eta_2 = \frac{G_{f12}/G_m - 1}{G_{f12}/G_m + \xi_2}$$

$$V_{12}^* = V_f v_{f12} + (1 - V_f) v_m$$

$$v_{23}^* = v_m \frac{1 + \xi_3 \eta_3 V_f}{1 - \eta_3 V_f}, \text{ with } \eta_3 = \frac{v_{f23}/v_m - 1}{v_{f23}/v_m + \xi_3}$$

Where ξ_1, ξ_2 and ξ_3 need to be determined so that predictions of the modified rule of mixture match the ply properties in the absence of damages. It is interesting to note that both the major Poisson's ratio and the through-thickness Poisson's ratio are not affected by damage, while the longitudinal, transverse, and in-plane shear stiffness are strongly dependent on the degree of damage in the fibre and the matrix.

4.10 Open-Hole Tension (OHT) specimen

The case of composite quasi-isotropic plate with notch is built and damage was expected to initiate at the edge of the hole. One half of the open-hole tension specimen is symmetrically built. Plate has dimensions of 100mm*50mm. Total thickness of the plate is 1.25 mm. Diameter of the hole is 10 mm.

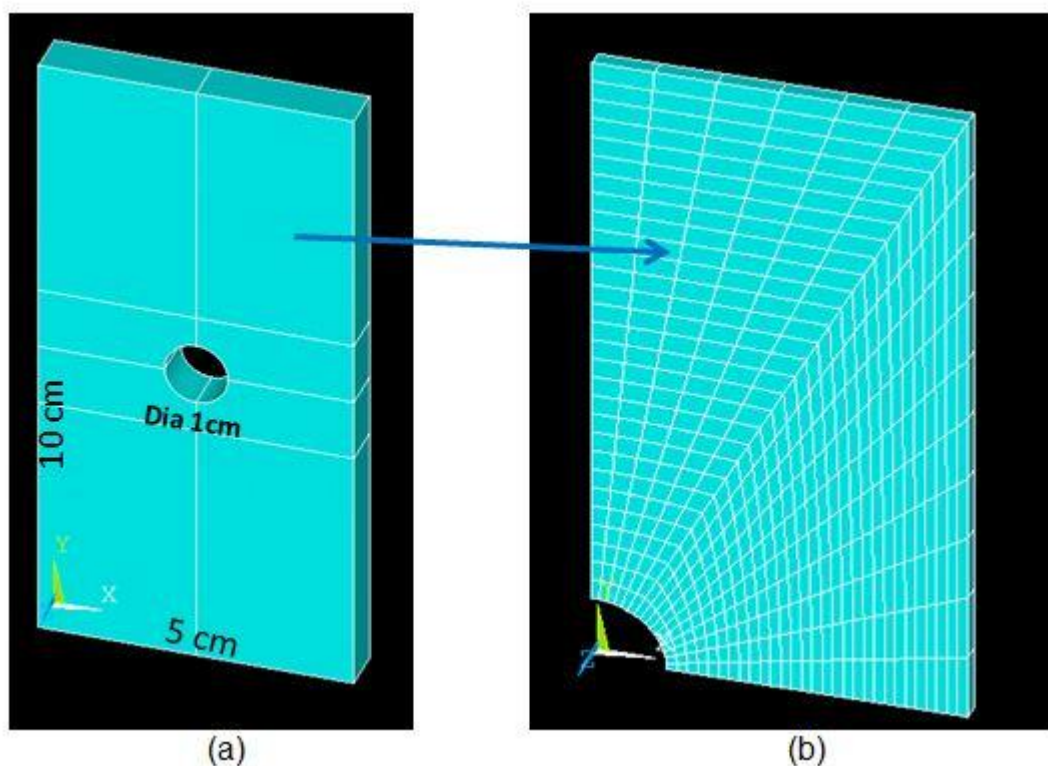


Figure 4.14 (a) open hole tension specimen (b) FE discretization of the quarter part of OHT specimen

Above figure shows open hole tension specimen model and its FE discretization. In the symmetry through-the-thickness, surface of symmetry is restrained so that it will not move laterally (out of plane). Unit displacement is prescribed as loading condition on the top of the plate. At the bottom, plate is restrained.

4.10.1 Damage progression in open hole tension specimen

The aim of research is to predict the damage in composite laminates. Damage progression in composite laminate can be predicted by using phase degradation approach and failure criteria used is Multi Continuum Theory.

MATLAB code was developed for phase degradation approach and MCT, and it also consists of transformation matrix which it will convert from global stress tensors to local stress tensors, it found four stress invariants to calculate the failure criteria equations from the local stress tensors, once equations satisfied then damage will initiate and propagate. Table 4.1 and Table 4.2 are given as an input to the Matlab code.

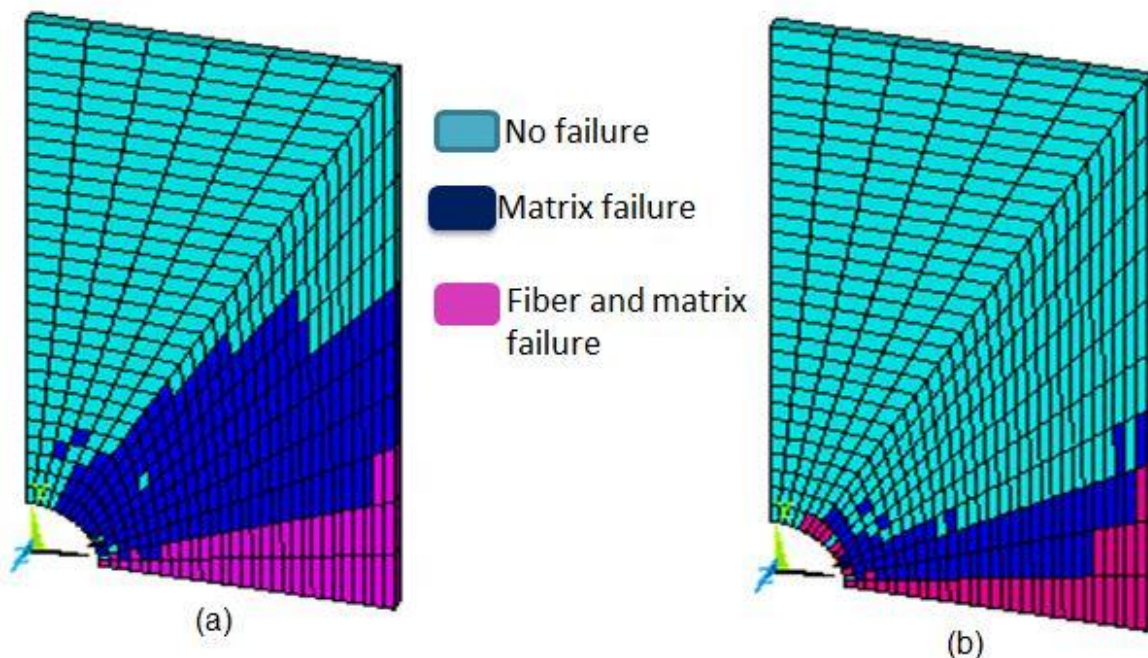


Figure 4.15 Damage progression for ply-1 and ply-2 of laminated composite (-30/30/-30/30) (a) 1st ply (30 deg) (b) 2nd ply (-30 deg)

Table 4.1 Matrix properties (3501-6)

Em(Gpa)	Gm(Gpa)	vm	+S22m(Mpa)	-S22m(Mpa)	+S33m(Mpa)	-S33m(Mpa)	S12(Mpa)
4.50	1.68	0.3	42.3	-176.3	5.52	-23.0	49.54

Table 4.2 Fiber properties properties (3501-6)

E11f(GPa)	E22f(GPa)	G12f(GPa)	G23f(GPa)	V12f(GPa)	V23f(GPa)	+S11f(MPa)	-S11f(MPa)	S12f(MPa)
207.5	25	95	9.20	0.24	0.359	3202	-2431	101

Above figure illustrate the predicted damage progression of each ply of laminated composite $[-30/30]_s$ when 144 elements are failed. Generally, the damage initiates at the right and left area close to the central hole. Ply-1 (-30 degree) has large amount of failed elements which are dominantly failed due to shear distortion.

4.11 Conclusion

In this chapter failure was predicted in masonry wall and also failure of composite laminate was predicted.

Discrete Masonry wall was modeled in Abaqus and individual isotropic properties of brick and mortar was used. The material model was used to predict the damage of the wall is Concrete damage plasticity in terms of plastic strains. Masonry will fail either due to tension or compression, so damage due to tension and compression were essentially form cracking strain and inelastic strains respectively, these strains will automatically convert to the plastic strains by the Abaqus. Due to plastic strains of masonry wall we can predict load vs. displacement plots beyond the yield.

In the second part of this chapter multiscale failure modeling of periodic composite was discussed. Here we are doing the analysis at macro level (e.g. OHT specimen) and we are seeing failure at micro level by using multi continuum failure theory and phase degradation approach. Here MCT and phase degradation approach was implemented in MATLAB programme.

Chapter 5

Conclusion

5.1 Conclusion and summary

In this study, effective properties or homogenised properties of masonry has been found from micromechanics RVE (representative volume element) analysis. Average theorems are used to found the effective properties of masonry. Average stresses and average strains are found from FE analysis, six numerical analysis are carried out to find the stiffness matrix and compliance matrix.

In this work we investigated the effects of mortar moduli on the homogenized equivalent material properties of the unit cell, the material properties of the brick are kept constant whereas the properties of the mortar are varied. Different stiffness ratios of brick to mortar are considered in the analysis and the plots of the ratios of Young's modulus of brick to Young's modulus of mortar (E_b/E_m) ranging from 1 to 1000 vs. the normalized homogenized equivalent Young's moduli and shear moduli (E_{eq}/E_b and G_{eq}/G_b) are made. Both (E_{eq}/E_b and G_{eq}/G_b) begin with the value of 1.0 when E_b is equal to E_m , and decrease rapidly at the beginning and then slowly increase of the modulus ratio E_b/E_m . E_{zz} is greater than the E_{xx} and E_{yy} , and In-plane shear modulus G_{xy} is also less than the out-of plane shear moduli G_{yz} and G_{zx} . These observations indicate that the unit cell has higher out-of-plane stiffness than its in-plane stiffness. Because of the out of plane stiffness G_{zx} is more, the in plane Poisson's ratio ν_{xy} is less.

Plots are also made for strengthen with CFRP and unstrengthen masonry, using the CFRP the out of plane shear modulus G_{zx} strength is becoming high compared to the other shear modulus values. And young's modulus E_{zz} , E_{xx} also showing high values compared to the E_{yy} modulus for the strengthen and unstrengthen masonries.

In the chapter 4 failures were predicted in masonry wall and also failure of composite laminate was predicted.

Discrete Masonry wall was modeled in Abaqus and individual isotropic properties of brick and mortar was used. The material model was used to predict the damage of the wall is Concrete damage plasticity in terms of plastic strains. Masonry will fail either due to tension or compression, so damage due to tension and compression were essentially form cracking strain and inelastic strains respectively, these strains will automatically convert to the plastic strains by the Abaqus. Due to plastic strains of masonry wall we can predict load vs. displacement plots beyond the yield.

In the second part of this chapter multiscale failure modeling of periodic composite was discussed. Here we are doing the analysis at macro level (e.g. OHT specimen) and we are seeing failure at micro level by using multi continuum failure theory and phase degradation approach. Here MCT and phase degradation approach was implemented in MATLAB programme.

References

- [1] Anthoine A. Derivation of the in-plane elastic characteristics of masonry through homogenization theory. *Solids Struct* 1995;32(2):137–63.
- [2] Zucchini A, Lourenco PB. A micro-mechanical model for the homogenisation of masonry. *Int J Solids Struct* 2002;39:3233–55.
- [3] Mistler.M,Anthoine.A. Inplane and out of plane homogenisation of masonry. *IntJ computers and structures* 85(2007); 1321-1330.
- [4] Abaqus, 2007, Abaqus Standard Reference Manuals, version 6.7. Simulia, Providence, RI, USA.
- [5] A. Zucchini, P.B. Lourenço A micro-mechanical homogenisation model for masonry: Application to shear walls. *International Journal of Solids and Structures* 46 (2009) 871–886
- [6] Anthoine, A., 1997. Homogenisation of periodic masonry: plane stress, generalised plane strain or 3D modelling *Communications in Numerical Methods in Engineering* 13, 319–326.
- [7] Lourenco, P.B., 1997. On the use of homogenisation techniques for the analysis of masonry structures. *Masonry International* 11 (1), 26–32.
- [8] Lourenço, P.B., 1996. *Computational Strategies for Masonry Structures*. Ph.D. Thesis, Delft University of Technology. Available from: <www.civil.uminho.pt/masonry>.
- [9] Pande, G.N., Liang, J.X., Middleton, J., 1989. Equivalent elastic moduli for unit masonry. *Computers and Geotechnics* 8, 243–265.

- [10] Aboudi, *Mechanics of Composite Materials - A Unified Micromechanical Approach*. North-Holland, Amsterdam (1993).
- [11] Zucchini, A., Lourenço, P.B., 2007. Mechanics of masonry in compression: results from a homogenisation approach. *Computer and Structures* 85, 193–204.
- [12] Zucchini, A., Lourenço, P.B., 2004. A coupled homogenisation-damage model for masonry cracking. *Computer and Structures* 82, 917–929.
- [13] Lourenço, P.B., Rots, J.G., 1997. Multisurface interface model for the analysis of masonry structures. *Journal of Engineering Mechanics, ASCE* 123, 660–668.
- [14] Shieh-Beygia, B., Pietruszczak, S., 2008. Numerical analysis of structural masonry: mesoscale approach. *Computers and Structures* 86, 1958–1973.
- [15] Tsai S.W., 'Theory of composites Design'. 1992: Think composites
- [16] J.S. Mayes and A.C. Hansen, "A comparison of multicontinuum theory based failure simulation with experimental results," *Composites Science and Technology*, vol. 64, Mar. 2004, pp. 517-527.
- [17] D. Kenik, "Advanced techniques for constituent-based progressive failure analysis of composite structures," Master's thesis, University of Wyoming, 2009.
- [18] R. Hill, *The Mathematical Theory of Plasticity*, London, England: Oxford University Press, 1950.
- [19] Z. Hashin, "Failure criteria for unidirectional fiber composites," *Journal of Applied Mechanics*, vol. 47, 1980, pp. 329-334.